Physics – Uspekhi **56** (2) 123 – 140 (2013)

REVIEWS OF TOPICAL PROBLEMS PACS numbers: **42.65.–k**, 42.65.Jx, 42.65.Ky, 42.65.Re, 52.38.Hb

From self-focusing light beams to femtosecond laser pulse filamentation

S V Chekalin, V P Kandidov

DOI: 10.3367/UFNe.0183.201302b.0133

Contents

Abstract. 2012 marked the 50th anniversary of the first published prediction of the self-focusing phenomenon in light beams. The recent revived interest in the subject is due to advances in high-power femtosecond laser technology and due to the possibility they provided of creating extended filaments of high light field intensity in gases and condensed media. This review shows in retrospect how our understanding of the self-action of light evolved from the self-focusing of laser beams in the 1960s to the filamentation of femtosecond laser pulses at present. We also describe the current status of this rapidly growing area of nonlinear optics and laser physics. Finally, we discuss, in general terms, what the phenomena of laser beam self-focusing and laser pulse filamentation have in common and how they differ.

1. Introduction. Self-action effects of laser radiation

The year 2012 marked the 50th anniversary of the publication of a paper by Askar'yan [1] in *JETP*, in which he predicted the self-focusing effect for laser beams. This jubilee is inseparably linked with the 50th anniversaries of the invention of lasers and the advent of nonlinear optics, which were celebrated in the preceding years. It was not until the making of lasers that the observation and use of numerous nonlinear optical effects were made possible. The self-focusing of light occupies a special place among these effects, because it gives rise to a wealth of other nonlinear effects due to the avalanche-like increase in the light energy density. A large contribution to the discovery of the self-focusing effect and its investigation was made by the Russian scientists A M Prokhorov, N G Basov, and R V Khokhlov, who represent the Moscow scientific school, and V I Talanov, who represents the school of Nizhny Novgorod.

The past decade has seen a revival of interest in light self-focusing. This is directly related to the development of high-power femtosecond laser facilities, which allowed producing extended filaments of laser radiation with a high energy density in gases and condensed media. The laser energy localization in the bulk of a medium without any guide systems, the production of plasma channels, the generation of broadband supercontinuum radiation, and the conical emission in laser filaments have rekindled interest in the study of optical radiation filamentation. Several reviews, special issues of scientific journals, and monographs have been published that are dedicated to the filamentation of laser radiation in different media and its application. We are particularly delighted to note that Russian researchers have also played a significant role at this stage. Femtosecond filamentation effects are at the heart of new laser technologies in ecology, biophysics, atmospheric optics, microoptics, and other areas.

Self-action effects emerge for high-power light waves [2, 3] because a significant contribution to the response of a medium, along with linear polarization, is made by nonlinear polarization, which is proportional to odd powers of the electric field strength. The physical reasons for the emergence of a nonlinear medium response are highly diversified. The degree of manifestation of one optical nonlinearity mechan-

S V Chekalin Institute of Spectroscopy, Russian Academy of Sciences, 142190 Troitsk, Moscow, Russian Federation
Tel. +7 (495) 851 02 37. Fax +7 (495) 851 08 86
E-mail: schekalin@yandex.ru
V P Kandidov Physics Department, Lomonosov Moscow State University, Leninskie gory, 119992 Moscow, Russian Federation
Tel. +7 (495) 939 30 91
E-mail: kandidov@physics.msu.ru

Received 14 February 2012, revised 30 March 2012
Uspekhi Fizicheskikh Nauk **183** (2) 133 – 152 (2013)
DOI: 10.3367/UFNr.0183.201302b.0133
Translated by E N Ragozin; edited by A M Semikhatov

ism or another is determined by the medium properties, as well as by the radiation characteristics like the pulse duration, transverse beam size, intensity, polarization, and wavelength. All the mechanisms underlying the nonlinearity can be divided into three categories, which correspond to different physical processes:

(i) the Kerr effect, electronic and orientational;

(ii) nonlinear polarizability, which is associated with the macroscopic transformation of the medium caused by its density variation in electrostriction, adiabatic, and isobaric thermalization of the absorbed light energy, as well as in the variation of the free carrier density under the action of a high-intensity light field;

(iii) resonance effects in amplifying or absorbing media associated with saturation.

We briefly discuss each of the main mechanisms separately.

• The electronic Kerr effect, which is caused by the nonlinear electronic polarizability of the atoms and molecules of a medium, is due to the deformation of their shell by the light field. Most significant in the nonlinear polarization in this case is its cubic dependence on the field. The contribution of the fifth- and higher-order nonlinearities in the self-action of laser radiation in gases has recently come under discussion [4]. However, no negative contribution of the higher-order Kerr nonlinearities was discovered in the direct measurements of nonlinear response in argon and nitrogen at intensities close to the ionization threshold intensity [5]. According to Ref. [6], the higher-order nonlinearity can suppress the beam self-focusing at an intensity lower than the threshold intensity for laser plasma production, which would qualitatively change the character of conical supercontinuum emission. At the same time, the existence of the fifth- and higher-order Kerr nonlinearities extends the possibilities for interpreting the supercontinuum generation in the self-focusing of light [7]. The characteristic nonlinear polarization response time in the electronic Kerr effect is equal to $10^{-15}-10^{-16}$ s. The orientational Kerr effect manifests itself in liquids consisting of molecules with an anisotropic polarizability or a static dipole moment, where the nonlinear polarizability emerges due to the so-called optical Kerr effect. Variations of the refractive index in this case, as in the case of the well-known static Kerr effect, result from molecular alignment with the field vector. A strong light field leads to the ordering of the anisotropically polarizable molecules, with the result that the medium becomes anisotropic and the refractive index becomes higher for the ordering field. The induced anisotropy is proportional to the light field strength squared. The characteristic relaxation time of molecular ordering is equal to $10^{-8}-10^{-9}$ s. This mechanism does not make an appreciable contribution for pulses shorter than 10^{-9} s. These nonlinearities are spatially local, and the nonlinear increment of the refractive index in the medium is proportional to the intensity. For a pulse of a duration longer than the nonlinearity relaxation time, the increment of the refractive index is expressed as $\Delta n_{\mathrm{Kerr}} = n_2 E^2$, where n_2 is the nonlinearity coefficient of the medium and E is the electric field amplitude in the light wave.

• The macroscopic density variation in the medium under the pressure induced by a strong light field can be caused by the electrostriction effect or by adiabatic expansion in the relaxation of the absorbed laser energy. This deformation is attended by a change in the density ρ of the medium and therefore in its permittivity and refractive index in the domain occupied by the beam, $\Delta n_\rho \approx (\partial n/\partial\rho)\,\delta\rho(E^2)$. The nonlinear response of the medium is spatially nonlocal because it is associated with the propagation of a sound wave along the beam cross section, and the characteristic transient period of the nonlinear polarization is equal to the ratio of the transverse beam size and the sound velocity. The mentioned effects are significant in the self-action of the pulse with a duration of the order of this characteristic time. The contribution $\Delta n_T \approx (\partial n/\partial T)\,\delta T(E^2)$ from the isobaric expansion of the medium to the nonlinear increment of the refractive index is determined by its dependence on the temperature T. In this case, the characteristic nonlinear response time is determined by the temperature relaxation in the beam section due to heat and mass transfer in the medium. The strictional, adiabatic, and isobaric nonlinearities are, to a first approximation, cubic in the field strength. The increment of the refractive index in the production of a laser plasma or the transition of electrons to the conduction band induced by a high-intensity light field is negative and proportional to the free carrier density, $\Delta n_{\mathrm{pl}} = -4\pi e^2 N_{\mathrm{e}}/(2m_{\mathrm{e}}\omega^2)$, where e and m_{e} are the electron charge and mass, and ω is the optical oscillation frequency. In the multiphoton ionization in gases and avalanche ionization in condensed media, the change in the refractive index is given by power and exponential functions of intensity. That is why the generation of free carriers is threshold in character for a high order of the multiphoton process. The nonlinearity can be regarded as being local for short pulses with diffusion of the carriers neglected. Its settling time is determined by the intensity for a specific carrier production process.

• In media with resonance amplification or absorption, the saturation effect is responsible, as is well known, for changes in the refractive index in the domain of anomalous dispersion. It is significant that the sign of the increment in the refractive index depends in this case on whether the radiation frequency is higher or lower than the resonance transition frequency in the medium.

1.1 Light self-focusing. Early studies

Light self-focusing is related to the laser beam wavefront distortion arising from a nonlinear increment in the refractive index of a medium in a high-intensity light field. When this increment is positive ($\Delta n > 0$), the refractive index for a Gaussian beam in its paraxial portion is greater than at its periphery, making the radiation phase velocity lower in the vicinity of the axis. Because optical rays propagate normally to the wavefront, they converge to the axis, and the beam experiences self-focusing for such a refraction, with a consequential avalanche-like increase in the axial intensity (Fig. 1). Indeed, even a small intensity increase in some domain of the cross section of a light beam in the medium with $\Delta n > 0$ results in the concentration of rays in this domain and therefore in an additional increase in intensity, which enhances the effect of nonlinear refraction. When the effect of self-focusing precisely compensates the diffraction beam spreading, this regime is referred to as self-channeling [2].

The term self-focusing was introduced by Askar'yan in his paper "Effect of the field gradient of a high-intensity electromagnetic beam on electrons and atoms" [1]. This work was concerned with the effect of plasma expulsion from a light beam by the gradient forces emerging in a high-intensity electromagnetic field and with the use of this effect for bulk heating of the plasma, its confinement in the beam, and production of "radiative plugs." In Ref. [1], the self-

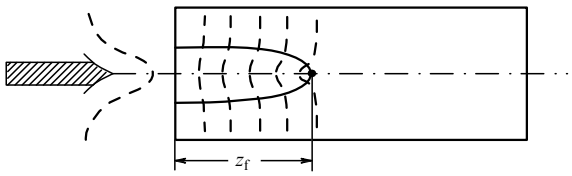

Figure 1. Wavefront curvature in a nonlinear medium, which is responsible for self-focusing [2].

focusing effect was predicted with only two phrases: "Therefore, the beam will force the plasma out of the volume of its field, which may lower the diffractive divergence." And at the end of the paper: "It is interesting to note that the ionizing, thermal, and separating action of a high-intensity radiation beam on a medium can be strong enough to produce a difference in the properties of the medium inside and outside of the beam, which will result in a waveguide beam propagation and eliminate geometric and diffractive divergences — this interesting phenomenon may be termed the self-focusing of an electromagnetic beam." This prediction was nevertheless recorded as discovery No. 67 with priority of 22.12.1961, which has the following description: "A heretofore unknown effect of self-focusing of electromagnetic and sound beams was discovered, which consists in a lowering of the divergence (or in an increase in convergence) of the beams due to the emergence of a lateral gradient of the nonlinear refractive index and the production of a nonlinear waveguide, which decreases the beam cross section." We note that Askar'yan's priority, despite the discovery registration, was not unanimously recognized for a long time. This nonrecognition was especially conspicuous, curiously enough, in Russian (then Soviet) science. Its causes and peripeteia were described in sufficient detail by Bolotovskii [8]. The situation has now changed, and the discovery of self-focusing by Askar'yan has been included in classic books on theoretical physics, while the phenomenon itself is described in monographs and textbooks on optics and nonlinear wave physics [2, 9–16].

In later papers, Askar'yan defined self-focusing as "the decrease in divergence (or the increase in convergence) of a high-power radiation beam due to different nonlinear effects induced by the beam itself." This definition was formulated after attempts were made to find the self-consistent intensity distribution for a light beam that would be invariable over a sufficiently long distance in a nonlinear medium. In 1964, such distributions were obtained by Talanov [17] for electromagnetic waves in plasmas and simultaneously by Chiao, Garmire, and Townes [18] for light beams. Theoretical paper [18] discussed the mechanisms of nonlinear polarization with different response times and investigated the mechanism of light beam self-trapping into a nonlinear waveguide produced by the radiation itself in a transparent cubic medium, the diffractive beam divergence being completely compensated by the nonlinear lens emerging in this case. Proceeding from these notions, the authors introduced the concept of the critical light beam power,

$$P_{\rm cr} = \frac{1.86}{32\pi^2}\frac{\lambda^2 c}{n_2} \qquad (1)$$

(where λ is the radiation wavelength and c is the speed of light in the vacuum), which is central to the effect of self-focusing, and estimated $P_{\rm cr}$ for different media.[1] For a cubic nonlinearity with an instantaneous response, it was possible to find a quasistationary solution of the nonlinear wave equation and to numerically determine the stationary amplitude profile of a self-channeling beam, which later came to be known as the Townes mode. In Ref. [23], it was shown that the self-focusing of the Townes beam is free from aberrations. The axially symmetric beam with the Townes mode profile underlies the physical interpretation of many experiments involving the self-focusing of light beams and the filamentation of femtosecond laser pulses. The authors of Ref. [18] obtained several highly important results and formulated several statements, which were not properly recognized at first, but were amply borne out later on. In particular, they hypothesized that a beam with an above-critical power can decay into several smaller beams of the threshold power, i.e., they made the first prediction of the effect of small-scale self-focusing. They pointed out that the low critical power of self-focusing in liquids can explain the anomalies observed in stimulated Raman scattering (SRS).

Interestingly, unlike Talanov's investigations [17], those in [18] were fostered not by Askar'yan's work [1], which predicted self-focusing and which the authors of Ref. [18] were then unaware of, but by the experiment on the observation of filamentary damage in glass produced in the focusing of a high-power beam of a ruby laser [24]. However, this experiment, which was reported to a conference in 1964, was far from the observation of self-focusing; furthermore, its author did not even suspect the very existence of such a phenomenon. Finally, as became apparent later, the filaments observed in Ref. [24] are hardly attributable to self-focusing, because, in the event of an optical breakdown in a medium, a distinctive spatio-temporal selection of filamentary laser radiation occurs [3]. Nevertheless, several papers, especially foreign, mention the experiment in Ref. [24] as the first observation of self-focusing. For instance, the first original publications on the self-focusing of light were reprinted in recent collected articles [25]; reprinted among these was a paper on the experiment in Ref. [24], which had previously existed only in the form of an abstract of a conference report.

In reality, the self-focusing of light was first recorded in [26] in experiments with the propagation of a 20 MW focused ruby laser beam in organic liquids. The authors of Ref. [26] gave a lucid physical interpretation for the self-focusing of a laser beam into a narrow filament as the effect of self-focusing of light predicted in Ref. [1] and theoretically investigated in Refs [17, 18]. Along with Ref. [26], we also mention the experiments of Lallemand and Bloembergen [27], also published in 1965, on the observation of anomalous amplification in SRS. In these experiments, using crossed polarizers, the authors observed bright micrometer-size spots on the cell end, which they attributed [26] to the self-focusing discussed theoretically in Refs [1, 17, 18].

Currently, there is no doubt that the self-focusing effect manifested itself in the majority of experiments where high-power light beams generated by Q-switched lasers propagated

[1] In Ref. [18], the critical power was defined up to a numerical factor. The inaccuracies that appeared in the history of its determination are discussed at length in Ref. [11]. The quantity $P_{\rm cr}$ defined by formula (1) [11, 19] is the critical power for the self-focusing of a collimated beam with a Gaussian profile. For beams with other profiles (asymmetric, in particular), the critical power is higher. A beam with the Townes mode profile has the lowest critical power [11, 20–22].

in liquids. From these experiments, it was possible to gain certain information about the self-focusing effect as such, in particular, to experimentally estimate the critical power $P_{\rm cr}$. In this case, however, only the consequences of self-focusing were observed, rather than the high-intensity light filaments themselves, unlike in Ref. [26].

In 1965, Kelley [28] introduced the notion of a self-focusing length (Fig. 1). Two years later, the following expression was obtained for the self-focusing length by generalizing the data of numerical simulations [29]:

$$z_{\rm f} = \frac{0.366ka_0^2}{\left[\left(\sqrt{P/P_{\rm cr}} - 0.825\right)^2 - 0.03\right]^{1/2}}\,, \qquad (2)$$

where a_0 is the beam radius, $k = (\omega/c)\,n$ is the modulus of the wave vector in the medium, and n is the linear refractive index. Interestingly, in 1975, expression (2) was reproduced with insignificant differences in Ref. [30] and, not quite justifiably, came to be known as the Marburger formula,[2] which is extensively used in English-language literature. Kelley [28] numerically determined the variation of a laser beam profile in the self-focusing and showed, using the quasioptical approximation, that a beam with an above-critical power experiences infinite contraction with an unlimited intensity growth at its center and profile transformation to the Townes mode profile.[3] This work also provided an explanation for the SRS anomalies observed in experiments with liquids. In 1966, Garmire, Chiao, and Townes [33] measured the self-focusing length by observing the laser beam evolution in the self-focusing in carbon disulphide and obtained good agreement with the formula derived in Ref. [28]. However, the beam contraction was observed until the beam diameter became smaller than 50 μm, after which the beam decayed into filaments 10 μm in diameter at a power much higher than $P_{\rm cr}$. The authors of Ref. [33] observed rings in the intensity distribution around the nonlinear focus, which is attributable to the interference of radiation trapped in the filament and the untrapped radiation or to higher modes of the nonlinear waveguide. They measured the critical power and the nonlinear increment of the refractive index and also determined that the nonlinearity-induced phase shift of the light field smoothly varied from the center to the beam edge, reaching $\pi/2$ [33].

The decisive role in the theoretical investigation of light beam self-focusing was played by the work of Akhmanov, Sukhorukov, and Khokhlov [3, 34], who obtained the solutions of quasioptical equations in the aberration-free approximation and estimated the critical power and the self-focusing length for Gaussian beams.

It is noteworthy that the first papers dedicated to self-focusing, beginning from the priority paper by Askar'yan, discussed the waveguide propagation mode, and its most promising application seemed to involve light energy transport over long distances without diffraction losses. However, even the first experimental and theoretical papers described above discussed the limitations of these conceptions. First, in the framework of the quasioptical approximation, attempts to explain not only the experimentally observed dimensions of filaments but also their splitting into smaller ones at a sufficiently high power (small-scale self-focusing) did not meet with success. Second, the same approximation suggested that the waveguide propagation mode of real light beams was highly unstable. Third, the powers required for the Kerr self-focusing could be achieved only in a pulsed regime, while all theoretical calculations were performed for the stationary case.

Khokhlov first noted the instability of a plane wave in a nonlinear dielectric in his talk at the First All-Union Symposium on Nonlinear Optics in Minsk (June, 1965) [35]. The spatial instability of a sufficiently intense light field with respect to small amplitude and phase perturbations, as well as with respect to small perturbations of the medium and the consequential beam decay into numerous separate fragments, i.e., small-scale self-focusing, were theoretically substantiated by Bespalov and Talanov (1966) [36], who first showed that there is a characteristic, the most rapidly focusing, transverse optical radiation scale length

$$\Delta x = 1.22\lambda\left(\frac{c}{32\pi n_2 I}\right)^{1/2}, \qquad (3)$$

which is defined by the radiation intensity I and the medium nonlinearity coefficient n_2.

The field strength of a laser pulse and therefore self-focusing length (2) vary in the course of the pulse. The time variation of the position of the nonlinear focus of a laser pulse was noted by McWane [37] in 1966, as well as by Marburger and Wagner [38] in 1967.

In 1967–1968, Dyshko, Lugovoi, and Prokhorov proposed the model of moving foci to explain the experimentally observed self-focusing filaments in laser pulses [39, 40]. The essence of the model is rather simple and physically lucid. The power of a pulsed laser beam varies with time in accordance with the envelope of the laser pulse. Because the position of the nonlinear focus on the beam axis depends on its power, the focus moves along the beam axis during the course of the pulse. For giant laser pulses, under typical conditions, the velocity of focus motion is of the order of 10^9 cm s^{-1}. As a result of foci motion, the side picture of beam propagation exhibits thin filaments — the tracks of foci motion. In the moving foci model, the transverse dimensions of the filaments observed are determined by the transverse foci dimensions, while the 'lifetime' of these filaments is determined by the foci transit time through the observation plane. The calculated transit time was about 10^{-10} s under typical conditions, which agreed nicely with the experimentally measured lifetimes of the filaments. It is pertinent to note that the calculations were performed assuming an inertialess nonlinearity, which is quite true for the nanosecond range of pulse durations.

In the first experiments, the moving foci model was confirmed by analyzing the spatio-temporal picture of damage tracks in sapphire in the self-focusing of nanosecond laser pulses [41] and by directly observing the motion of the nonlinear foci of picosecond pulses in organic liquids [42, 43]. The moving foci model is obviously at variance with the conception of the waveguide propagation mode, which prevailed initially.

The theory of transient self-focusing of a laser pulse whose duration is comparable to the characteristic settling time of

[2] The Marburger formula: $z_{\rm fil} = 0.367ka_0^2/\left\{\left[(P_{\rm peak}/P_{\rm cr})^{1/2} - 0.852\right]^2 - 0.0219\right\}^{1/2}$.

[3] As shown in Ref. [31], in a more rigorous description of the beam diffraction taking the longitudinal 'diffusion' of the complex amplitude and the longitudinal component of the light field into account, the beam radius and the intensity are finite at the nonlinear focus. This is borne out by the direct solution of the Maxwell equations for the self-focusing problem of a light beam [32].

the nonlinear polarization in a Kerr medium was developed in Refs [2, 34]. In these papers, it was shown that because of the retardation of the nonlinear response, self-focusing is experienced by the 'tail' of the pulse, which leads to its symmetry breaking and envelope modulation.

Theoretical investigations of the self-focusing of polarized light beams, first performed in Ref. [44], subsequently showed that regimes are possible with both monotonic and nonmonotonic variation of the width of circularly polarized partial beams [45]. The critical powers defining different self-focusing regimes of circularly polarized light were determined in Ref. [46]. The focusing of one partial beam and the defocusing of the other one, with the effect that the total intensity distribution loses its Gaussian shape and the polarization becomes nonuniform are possible in an isotropic medium with a cubically nonlinear spatial dispersion [47]. In a medium where the components of the local nonlinear susceptibility tensor have opposite signs, several annular domains can emerge with right and left directions of rotation of the electric field strength vector [48]. Under the conditions of anomalous frequency dispersion, pulsed radiation decays into fragments with opposite directions of rotation of the electric field strength vector, each fragment having a nearly circular polarization [49–51].

1.2 Spectrum transformation under self-focusing

From 1966–1970, several experimental and theoretical studies were made to investigate the transformation of the pulse spectrum and hence of the temporal pulse shape due to self-action effects. In 1966, Bloembergen and Lallemand [52] observed a symmetric spectrum broadening of several dozen angstroms in the self-focusing of a giant pulse in carbon disulfide; they ascribed this effect to stimulated Raman scattering and Rayleigh scattering. Later, Shimizu observed an asymmetric spectrum broadening in carbon disulfide in the self-focusing of giant pulses with a picosecond envelope modulation [53]. Shimizu believed that the main mechanism of the broadening consisted in the self-modulation effect, which gave rise to a periodic spectrum structure. In that case, the substantially greater broadening towards the Stokes domain was attributed to the finite nonlinearity 'lifetime', i.e., to the response inertia. The calculations by Joenk and Landauer [54] pointed to another consequence of the finiteness of the nonlinearity relaxation time in a medium — to pulse shape distortion: the lengthening of the pulse leading edge and the self-steepening of the pulse trailing edge, whereby so-called envelope shock waves are produced.[4]

In the first experiments with picosecond pulses focused into optical crystal and glass samples, Bondarenko, Eremina, and Talanov [57], and Alfano and Shapiro [58, 59] recorded a superbroadening of the spectrum, so-called supercontinuum generation. For borosilicate glass, the increase in the spectrum width in the Stokes domain amounted to 4000 cm^{-1} and in the anti-Stokes domain to 7000 cm^{-1} [57], and to more than an octave [58, 59] in the absence of filamentary damage to the samples. The observed asymmetric frequency broadening of the pulse spectrum and the emergence of a periodic structure in the spectrum was interpreted as a consequence of the phase self-modulation [53] due to the electronic component of the Kerr nonlinearity [60]. These experiments revealed the angular divergence of the supercontinuum radiation and its increase with an increasing shift of the spectral components to the blue side (the halo of conical emission).

The decisive role of self-focusing in spectrum broadening was already noted in experiments in 1967 [53]. The occurrence of self-focusing filaments was found to unambiguously correlate with the superbroadening of the spectra of ultrashort pulses in liquids and glasses [61]. The subsequent experiments in Ref. [62] with picosecond pulses with wavelengths of 1.06 and 0.53 μm focused into water and heavy water cells also showed that supercontinuum generation is possible when the peak pulse power exceeds the critical self-focusing power. The influence of the laser-induced plasma on the pulse spectrum broadening in gases is weak according to Refs [63, 64], and it reveals itself in the anti-Stokes shift of the spectrum.

A broadband supercontinuum pulse, which extends from the ultraviolet to the near-infrared domain and is of the same order of magnitude in duration as the exciting pulse, was first used by Alfano and Shapiro [65] in experiments involving a pump–probe scheme, which has gained wide acceptance. The supercontinuum is a promising source for information transfer systems, laser probing, and other laser-based technologies.

2. Self-focusing in amplifying media

Apart from the study of the self-focusing effect itself, a prominent place was occupied by investigations of the influence of self-focusing on the characteristics of laser pulses in their amplification. This problem inevitably arose in the fundamental and practically important task of increasing the power of laser systems. Despite the critically important role of self-focusing in the amplification of high-power pulses, not many experiments were done on this subject, which was noted, in particular, in the well-known book by Shen [2]: "Strange as it may seem, few investigations have been done on self-focusing in an amplifying medium to date." True, this phrase is commented on by the editor of the translation, S A Akhmanov, who provided references to the 1971–1979 work carried out at the Lebedev Physical Institute (FIAN) and the Vavilov State Optical Institute (GOI).

It is evident that the specific character of self-action effects in amplifying media should manifest itself primarily for sufficiently high intensities of laser radiation. Clearly, the influence of these processes is especially strong in the generation and amplification of ultrashort pulses (USPs).

2.1 Self-action effects in ultrashort-pulse generators and femtosecond lasers (KLM lasers)

Early in the development of the generation technique of high-power USPs, neodymium glass lasers with a nonlinear absorber were practically their only source. USP generation in these lasers was best explained by the fluctuation theory by Letokhov [66], Kuznetsova [67], and Fleck [68]. According to this theory, USP generation is a probabilistic process involving the extraction of the highest light pulse from a random realization containing a multitude of fluctuation spikes. Theoretical calculations showed that a strong discrimination by a nonlinear absorber at the oscillator output had to give rise to a regular sequence of single USPs separated from one another by the cavity round-trip time (the cavity transit time). In this case, the ratio between the main pulse

[4] Attention to the formation of envelope shock waves in a nonlinear medium with a response delay was first drawn by Ostrovskii in Refs [55, 56].

amplitude and the amplitude of low-intensity background USPs (the radiation contrast ratio) for an oscillator operating in the principal transverse mode must be of the order of 10^6 [66]. However, numerous different experiments have suggested that the contrast ratio does not exceed $10^2 - 10^4$, even when oscillators with one transverse mode are used. It turned out that the main reason for such a significant disagreement lay with the nonlinear interaction of high-power USPs with the optical elements of the cavity, which was not included in the theory.

Treacy [69] was supposedly the first to observe the manifestation of self-action in neodymium glass USP generators in 1968: he recorded the emergence of a positive frequency shift (chirp) in the course of lasing and attributed it to the effect of phase modulation. Treacy also managed to compensate the observed chirp using a pair of diffraction gratings, thereby shortening the pulse duration. This technique is now used in all femtosecond pulse amplification facilities.

In earlier experiments, Glenn and Brienza [70] discovered a decrease in the conversion coefficient to the second harmonic in a USP train as it developed in a neodymium glass oscillator. They attributed the observed effect to the gradual lengthening of the pulses in the train without further explanation. In Refs [71, 72], this decrease in the conversion coefficient was explained in terms of the emergence of additional pulses unresolved by the photocell and the oscilloscope used to record picosecond pulses in Ref. [70]. In experiments with a picosecond time resolution, the emergence of additional pulses in the course of the USP train development, which is inexplicable in the framework of the fluctuation mechanism, was indeed observed by Korobkin, Malyutin, and Shchelev [73, 74]. In Ref. [75], this effect was attributed to the increase in importance of the role of nonlinear losses (NL) due to self-focusing in the optical elements of the oscillator upon increasing the intensity of USPs in the course of their development. Because of the NL, the highest-intensity pulses cease to undergo amplification and to contract faster than the others, i.e., the effect is opposite to the effect of a nonlinear absorber. In this case, an increase occurs in the amplitudes of the background and of weak satellites, especially of those that follow immediately after the main pulse, which bleaches the nonlinear absorber. The amplitude of the peak observed with an oscilloscope is proportional to the total energy of the main pulse and all additional pulses in the range of the time resolution of the instrument. Evidently, due to the nonlinear nature of the process, the conversion efficiency to the second harmonic is higher for a single pulse than for a group of pulses with the same total energy. To estimate the NL effect on the generation, the authors of Ref. [72] proposed the idea of measuring the variation of the conversion coefficient to the second harmonic along the USP train, which was experimentally realized for different energy densities in the cavity.

In several subsequent studies, it was discovered that USPs acquire an irregular shape, which changes from pulse to pulse in the sequence. By directly recording the temporal radiation structure of a neodymium glass USP oscillator with the use of a "picokhron" streak camera with a subpicosecond temporal resolution, the authors of Ref. [76] showed that smooth pulses with a half-amplitude duration of 5 ps were generated at the beginning of the pulse train. In the course of train development, the pulses were observed to change shape due to theoretically predicted self-action effects, specifically, a

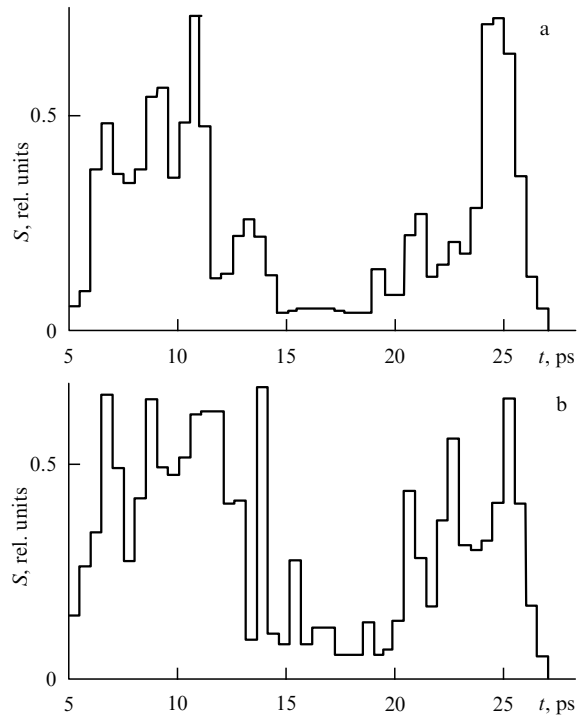

Figure 2. Photometric measurement data of a USP observed at the end of a pulse train with the help of a picokhron [76]. Shown is the same pulse recorded in two different channels (with a small delay in the case of Fig. 2b). *S* is the optical (photometric) density.

leading edge smoothing and a self-steepening of the trailing edge. Furthermore, the pulses acquired an irregular temporal structure: dips appeared in the envelope (Fig. 2), and the pulse width at the base significantly increased (in the presence of such a substructure, it is hard to speak of a half-amplitude pulse duration). The main conclusion drawn from the experiments in Ref. [76] was that the observed pulse transformation picture could not be explained by the fluctuation nature of the pulses, because the observed structure was hardly related to the manifestation of the 'background' observed in the emission at the initial stage: it developed from the initially smooth pulses as a result of some nonlinear processes.

Korobkin, Malyutin, and Prokhorov [77] ascertained two main reasons for the emergence of NL in USP oscillators: self-focusing and self-modulation of the pulse amplified in active elements. The former effect leads to a geometric energy loss due to an increase in its divergence, and the latter is responsible for the loss due to broadening of the spectrum beyond the amplification band. With the help of a streak camera, it was possible to experimentally record the variation of the spatial structure of the laser beam as well as of the pulse spectrum in the course of lasing development. In this case, the pulse spectrum acquired a regular structure characteristic of self-modulation in the glass of the active elements.

However, the mechanism responsible for the formation of the fine structure of the temporal USP profile that develops from a smooth pulse in the course of lasing was still unclear.

Zherikhin et al. [78, 79] proposed the following mechanism for the formation of an irregular temporal USP structure due to the nonlinear self-action in the active medium. In an active medium (a glass matrix), as the USP power increases, a nonlinear increment of the refractive index appears, which is

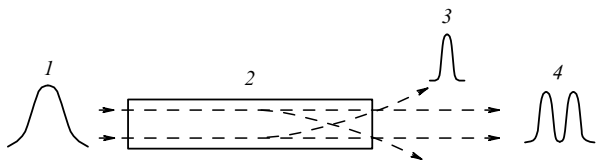

Figure 3. USP shape variation due to self-focusing in an active medium. *1* — input pulse, *2* — amplifying medium, *3* — scattered pulse, *4* — output pulse [78].

responsible for self-focusing. Its emergence mechanism is virtually inertialess, and initially the self-focusing of only the central part of the pulse, in which the intensity is maximum, occurs. The self-focusing results in the light scattering into a wide angle, thereby deflecting it out of the cavity aperture defined by the intracavity aperture. The scattering of the highest-intensity portion of a USP makes a dip in the pulse envelope (Fig. 3). The repetition of this process in the sequential passage of the USP through the oscillator cavity gives rise to an irregular USP structure. A similar pulse decay also occurs due to self-modulation, whereby the spectrum becomes wider than the amplification band. In this instance, however, the pulse envelope cannot fall to zero, which is the case in self-focusing.

Based on the proposed model, the transformation of the temporal USP structure was calculated for both an oscillator and a stable two-component medium [78, 79]. At the first stage, the pulse shape in the oscillator was assumed to vary due to self-focusing in the active element, which increased the beam divergence and therefore the loss under the limitation of the light beam by the intracavity aperture. In this case, the effects of the nonlinear absorber, the dispersion of the active medium, the finiteness of the amplification band, and the diffraction on the aperture were neglected. The active medium was replaced with a thin lens with a focal distance defined by the radiation field intensity in accordance with formula (2). Despite the rather crude assumptions made in this calculation, the character of variation of the USP shape, the train envelope, and the conversion coefficient to the second harmonic corresponded to those observed in experiments. At the second stage, a numerical method was used to obtain the transformation of the temporal distribution of the light field amplitude in the active medium of a ring oscillator used in experiments [79].

The analysis was performed in the approximation of slowly varying amplitudes with the inclusion of radiation self-focusing and self-modulation in the active medium, as well as of the effect of dispersion of the active medium and the profile of the amplification line:

$$\frac{\partial E}{\partial z} = \frac{\mathrm{i}}{2}\,\frac{\omega n_2 |E|^2 E}{cn} - \frac{\mathrm{i}}{2}\,\frac{\mathrm{d}^2 k}{\mathrm{d}\omega^2}\,\frac{\partial^2 E}{\partial t^2} + \frac{g}{\Delta\omega^2}\,\frac{\partial^2 E}{\partial t^2} + \left(g - \frac{\beta(z)}{b(z)}\right) E\,, \tag{4}$$

$$\frac{\mathrm{d}b}{\mathrm{d}z} = \beta(z)\,, \tag{5}$$

$$\frac{\mathrm{d}\beta}{\mathrm{d}z} = \frac{4 n_2 |E|^2}{n b(z)}\,, \tag{6}$$

where E is the complex amplitude of the light field, ω is the laser radiation frequency, n is the refractive index of the active medium, $n_2|E|^2$ is the nonlinear increment of the refractive index, $\Delta\omega$ is the amplification bandwidth of the active medium, g is the gain coefficient at the peak of the line, $\beta(z)$ is the angular beam divergence, $b(z)$ is the beam aperture, t is the time, and k is the magnitude of the wave vector. Equation (5) describes the variation of the beam aperture due to beam divergence and Eqn (6) shows the variation of the beam divergence $\beta(z)$ under the action of self-focusing.

The solution of Eqns (4)–(6) determined the pulse shape, its total energy, and the parameter η, which coincided, up to a constant factor, with the conversion coefficient to the second harmonic:

$$\eta = \frac{\int_T P^2(t)\,\mathrm{d}t}{\left|\int_T P(t)\,\mathrm{d}t\right|^2}\,,$$

where $P(t)$ is the instantaneous pulse power and T is the cavity round-trip time. For comparison, the calculation was performed both with the inclusion of self-focusing [system (4)–(6)] and without it [system (4), (5)] for the same initial conditions. In the former case (Fig. 4), the USP train envelope is nonmonotonic in character, the USP amplitude ε varying in antiphase with the conversion coefficient η to the second harmonic, in agreement with experimental data. With an increase in the number of transits, the pulse acquires a temporal structure that varies from transit to transit. In this case, the pulse shape is in good agreement with that observed with the picokhron (see Fig. 3). Without the inclusion of self-focusing (Fig. 5), the train envelope and the η parameter vary monotonically, the pulse shape varies much more slowly with the number of transits, and the pulse itself does not decay into shorter fragments. This comparison confirmed the prevalent role of self-focusing in the pulse decay into fragments, and the agreement between the calculated and experimental data confirmed the validity of the proposed model.

In parallel with this calculation, experiments were made to observe the USP train envelope in the direction of the cavity axis and that scattered forward in the angular range from 2.5° to 8° relative to this axis. Both envelopes were nonmonotonic, the dips in the envelope of the axially directed pulse train corresponding to the maxima of the envelope observed at an angle to the axis. This was direct evidence of the scattering loss due to beam self-focusing in the active element. Estimates based on these experimental data suggested that up to 10% of the beam energy was scattered in the indicated angular interval. The scattering to a solid angle of 2.5° was stronger by nearly an order of magnitude, supposedly because of the amplification of scattered light in the active medium. Backward scattering turned out to be 20 times less intense. Dedicated experiments also showed that the scattered light spectrum was strongly broadened.

These experiments allowed drawing the following main conclusion. In the course of USP generation, self-focusing in the active medium not only impairs the contrast ratio but also results in the decay of USPs into short fragments, whose duration lies in the femtosecond range. It was suggested to let this irregular-structured pulse pass through a stable two-component medium consisting of an amplifier and a nonlinear absorber in order to separate a single pulse and further shorten its duration. This has been possible to experimentally realize and obtain a single USP several hundred femtoseconds in duration [78]. However, this system turned out to be rather bulky and insufficiently stable.

In another method, it was planned to use a pulse that was cut out from the central part due to self-focusing in the active

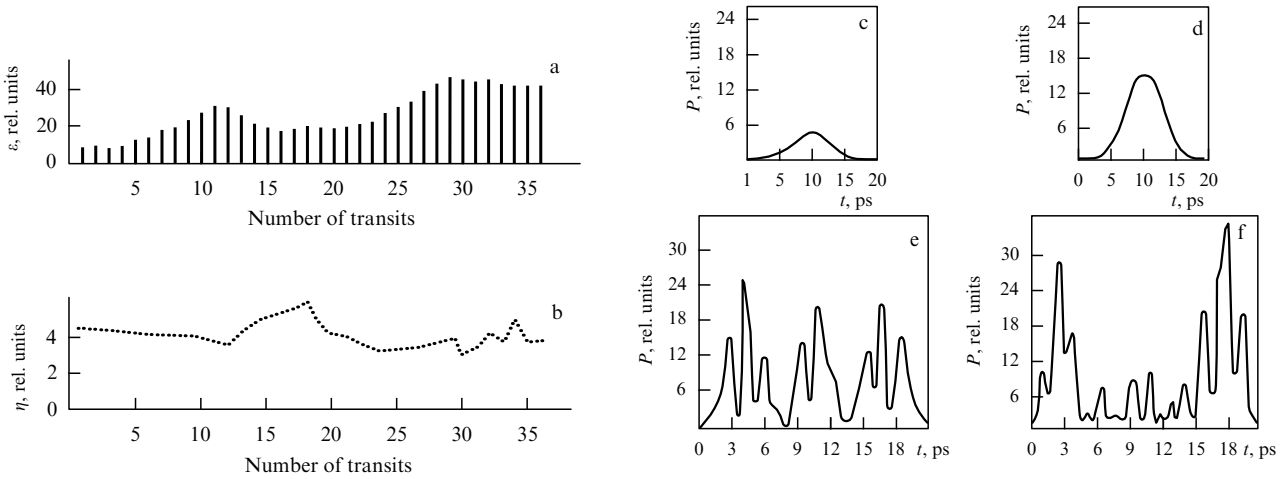

Figure 4. Results of the solution of system (4)–(6). (a) The USP energy ε and (b) the conversion coefficient to the second harmonic η calculated as functions of the number of cavity transits. (c) Variation of the initial pulse shape after (d) 10, (e) 25, and (f) 35 transits [79].

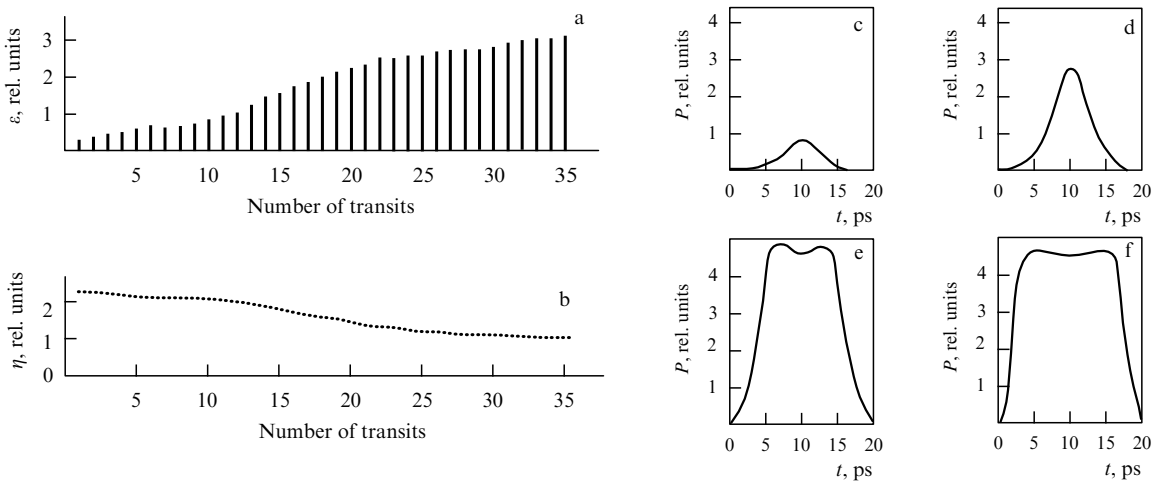

Figure 5. The same as in Fig. 4, but for solutions of system of equations (4), (5).

element, and thereby acquired a higher divergence, i.e., actually the laser radiation that went beyond the cavity aperture and was lost in the ordinary oscillator scheme (Fig. 3). In this case, the cavity must be designed so as to substantially lower the loss in the case of the light that diverges due to self-focusing in comparison with the loss in the case of the radiation that does not undergo self-focusing. Clearly, only one pulse can develop in such a cavity, and it subsequently shortens due to the repetition of self-focusing in successive transits through the oscillator cavity.

Almost two decades later, in 1991, a titanium–sapphire laser of this type was put into operation by Sibbett and collaborators in the USA. In their first publication [80], the mechanism of femtosecond pulse generation was in no way discussed. Sibbett used the standard commercial scheme employed for generating cw broadband radiation with titanium–sapphire, which had a very broad amplification band, and supposedly came across the femtosecond regime. A significant advantage of this scheme was that like all femtosecond oscillators, it was continuously pumped, and therefore a quasicontinuous sequence of USPs, and not a giant pulse, was generated in the stationary regime. It is pertinent to note that the generation of a regular sequence of USPs in a ruby laser without any Q-switching had also been observed previously.

The method of generating femtosecond pulses with the help of self-focusing in the active element, which was used by Sibbett, received the name Kerr-Lens Mode-locking (KLM) in subsequent papers [81]. The KLM titanium–sapphire laser has become the workhorse for the generation of femtosecond pulses in all modern laser facilities (sometimes referred to as third-generation lasers [82]), including superhigh-power petawatt lasers [83]. Therefore, the effect of self-focusing eventually played the decisive positive role in the development of modern femtosecond lasers. As regards its role in the amplification of USPs to obtain limit power levels, here the development of events was more dramatic.

2.2 Self-action effects in ultrashort-pulse amplifiers and output amplifiers of high-power femtosecond laser systems (CPA systems)

The first experiments to investigate the effect of the nonlinear loss related to self-focusing in USP amplification were performed simultaneously with the making of high-power multistage laser facilities. Interestingly, in these experiments,

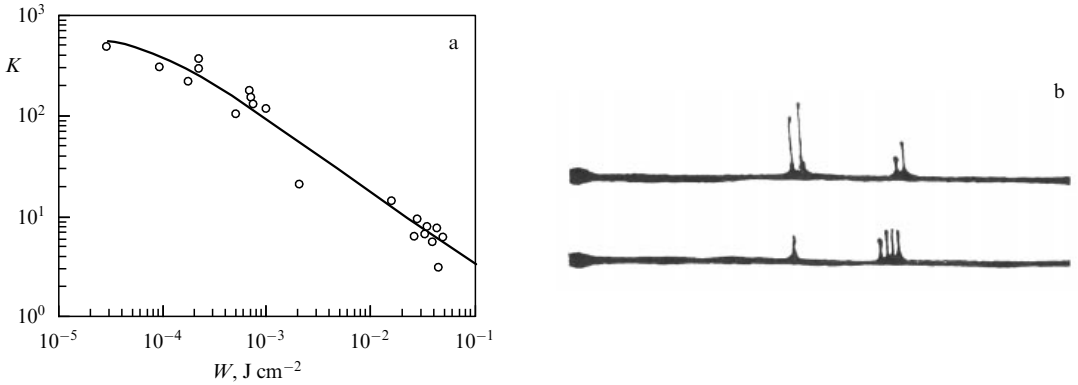

Figure 6. (a) The amplification factor K as a function of the input signal energy density W. (b) Emergence of additional pulses in the temporal structure of amplified radiation due to NL (the lower oscillogram). The upper oscillogram shows the input and output signals for a low input energy density. The time interval between the pair of pulses is equal to 8 ns [71, 85].

for a laser beam emanating from a multistage neodymium glass amplifier, it was for the first time possible to observe self-focusing in the air, which was recorded as an anomalously small beam divergence in an open 25 m long path [75]. Much filamentary damage to the active elements themselves was discovered later on. Experiments showed that several irregularly arranged filaments were produced in one shot in the output stage of a high-power amplifier. This was due to a significant excess over the self-focusing threshold and testified to the occurrence of small-scale self-focusing (SSSF) of a weakly diverging beam in the glass of the active elements [75].

Observed in subsequent experiments [84, 85] was an output beam halo with a divergence 3–4 orders greater than that of the main beam. The energy fraction contained in the halo increased steeply with increasing the power and became comparable to the energy of a directed laser beam. Measurements at the input and output of the energy of a laser beam with the divergence no worse than 5×10^{-4} rad showed that the amplification factor decreased by more than two orders of magnitude as the input energy density increased from 10^{-4} to 10^{-2} J cm^{-2} (Fig. 6a).

A natural consequence of the amplification nonlinearity detected was the impairment of the contrast ratio and the appearance of additional pulses at the amplifier output, which were not observed at the input, with increasing energy (Fig. 6b). Additional pulses were also present in the oscillator output, but their intensity was very low. It is worthy of note that the energy density at the amplifier output (~ 1 J cm^{-2}) was significantly lower than the gain saturation energy density for neodymium glass, and therefore the observed nonlinearity had a different nature. The power limitation in USP amplifiers was attributed to the loss and damage in optical materials caused by self-focusing in the active medium. Hence followed a practically important conclusion: because a sufficiently long medium was required for the development of self-focusing, it was desirable to obtain the needed amplification factor on the shortest possible length of the active medium.

An endeavor to weaken the influence of self-focusing on power limitation in amplifying stages was undertaken in Refs [84, 85]. First, an yttrium–aluminum garnet was used as the active medium in the USP oscillator. Owing to its high gain coefficient 0.1–0.2 cm^{-1}, which is higher than for neodymium glass by about an order of magnitude, lasing develops in a considerably smaller number of cavity transits than with a similar glass oscillator. Furthermore, the garnet has a narrow gain linewidth (≈ 1.5 cm^{-1}), which underlies the stable lasing of a longer (25–30 ps) and therefore lower-power pulse. In combination with the short length of the active element, this had the effect that self-focusing did not have time to significantly affect the structure of USPs during their development time. As a result, a smooth pulse with a transversely uniform field distribution was observed at the oscillator output. The conversion coefficient to the second harmonic was the same for all pulses of the train, which confirmed that the NL exerted no effect on the structure of the generated USPs.

Second, due to an additional cavity mode selection, the oscillator pulse duration was increased to 100 ps to lower its power in amplification experiments. For a first-stage amplifier, a 90 mm long yttrium–aluminum garnet active element 11 mm in diameter was used, which provided a very large amplification factor (≈ 500 per pass). Small-scale self-focusing could hardly develop in this element because with a high gain coefficient and, accordingly, a rapid growth of the pulse intensity with amplification, the scale of highest-increment perturbations, which is defined by the pulse intensity in (3), varies so rapidly that the perturbation self-focusing does not develop.

In such a system, it has been actually possible to eliminate SSSF both at the garnet amplifying stage and at the next double-pass 630 mm long amplifying stage of neodymium glass [84, 85]. However, the large-scale self-focusing of the beam as a whole, which was observed in both stages, had the effect that the output signal vanished completely. In this case, using a diverging beam, for which the self-focusing length

$$z_{\mathrm{f}'} = \frac{ka^2}{(P/P_{\mathrm{cr}} - 1)^{1/2} - ka\beta(z)} \tag{7}$$

for given radius a and power P depends on the angular divergence $\beta(z)$, proved to be a highly effective measure to eliminate large-scale self-focusing. To suppress large-scale self-focusing, the beam divergence should satisfy the inequality

$$\beta(z) \geqslant \frac{(P/P_{\mathrm{cr}} - 1)^{1/2}}{ka} \,. \tag{8}$$

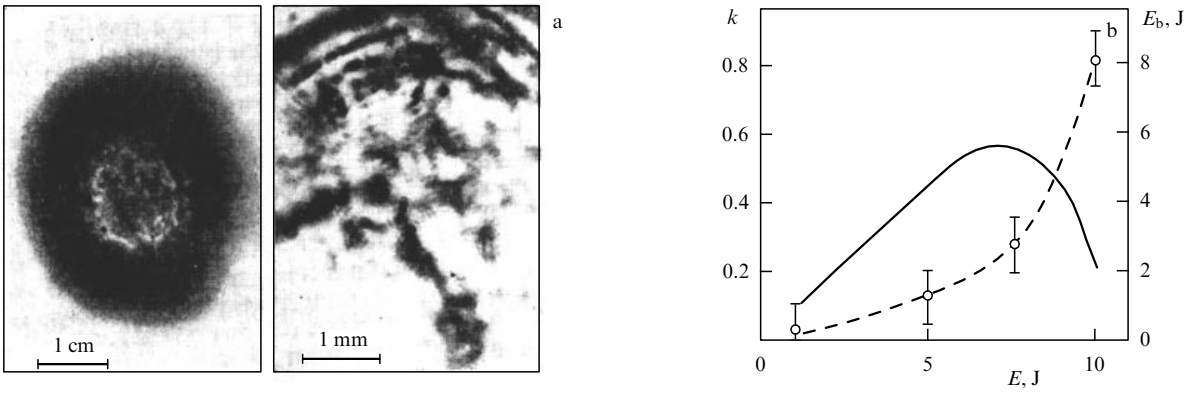

Figure 7. (a) Laser beam imprints on photographic paper at the facility output. (b) The relative energy $k = E_h/E$ of the halo (dashed line) and the energy of the collimated beam $E_b = E - E_h$ (solid line) as functions of the total pulse energy E at the facility output [84, 85].

In practice, it turned out that the highest energy could be achieved with an amplifier without wavefront distortion when the output beam diameter was twice the input one. Based on these considerations, a negative lens with a focal length of 30 cm was placed in front of the garnet. The garnet amplifier increased the pulse energy to $(2-4)\times 10^{-2}$ J, i.e., by a factor of 200–400. The pulse then passed twice through a neodymium glass amplifier, in which the beam diameter grew from 6 mm at the input to 12 mm at the output, and the energy increased to 0.5 J. No distortions of the laser beam were observed up to intensities of 3–5 GW cm^{-2}.

Upon a further intensity increase in the next amplifying stages, the transverse beam structure acquired small-scale rippling. On further amplification, these small-scale ripples transformed into many 'hot spots', each of which contained a power equal to three to five critical self-focusing threshold powers. The emergence of numerous irregularities in the transverse section of the output beam was attended by the appearance of a scattered radiation halo with a divergence far exceeding the initial beam divergence, which was equal to 5×10^{-4} rad. As the total output energy increased, the number of irregularities and the fraction of energy in the halo increased (Fig. 7). The energy and intensity at the amplifier output varied nonmonotonically to reach the peak values 5.6 J and 10^{10} W cm^{-2}. The indicated effects were not accompanied by damage to the active medium, which occurred only for energy densities higher than 1 J cm^{-2}, when the amplified radiation brightness showed a significant decrease.

The beam decay to a large number of hot spots is a typical manifestation of SSSF initiated by irregularities in the active medium. The mechanism of loss growth due to SSSF is supposedly as follows. The size of irregularities with the highest growth rate under conditions of the Kerr nonlinearity of the active medium and the development path length of their initiated SSSF decrease as the pulse energy increases. At the amplifier output, the number of hot spots emerging due to SSSF and their total energy increase, and hence the energy of the pulse that diverges upon self-focusing in the active medium becomes much higher.

The output laser energy can be divided into two parts: the main one is collimated, with a divergence of 5×10^{-4} rad, and passes through the amplifiers without wavefront distortion, and the other part forms a halo as a result of SSSF. The halo divergence is determined by the amplifier geometry, while the major contribution to its energy is made only by the part of the radiation that underwent SSSF and acquired a large divergence upon passing through nonlinear foci and which was next amplified in the active element. The beam brightness increases under amplification until the increase in the energy confined in small-scale irregularities, which next goes to the halo, becomes greater than the total increase in the beam energy. The use of a diverging beam to suppress SSSF turned out to be ineffective because the intensity value corresponding to the onset of SSSF is the same as that for a collimated beam.

Experiments also showed that a beam ceased to contract as a whole under SSSF. Therefore, small-scale irregularities in the medium are similar to a defocusing raster, as proposed by Askar'yan for eliminating large-scale self-focusing [86].

We note that self-focusing is responsible not only for a decrease in brightness but also for changes of the spatio-temporal radiation shape, because peripheral regions of the beam section experience much smaller distortions than the high-intensity paraxial domain, and the leading and trailing edges of a pulse also experience weaker distortions in comparison with its central part: owing to the small response time of the Kerr nonlinearity in glass, the refractive index increment is proportional to the intensity, which peaks at the pulse center on the beam axis [12, 85, 87].

All developers and users of ultrahigh-power facilities have encountered evidence of the fatal role played by self-focusing. Always observed in amplifiers, along with wavefront distortions, was a very strong broadening of the amplified pulse spectrum, which extended beyond the amplification band due to self-modulation in the active medium and led to significant losses. But these losses did not compare with the geometrical losses due to SSSF, which became a real curse for all researchers who endeavored to amplify the laser pulse power to record high values. This effect has always set the limit on the power attainable in a given facility: a further increase in the amplification factor becomes senseless and harmful. To quantitatively describe the self-focusing in real laser systems, where the beam intensity I varies along the optical path, as do the properties of the optical medium itself, the so-called decay integral, or the B integral is used [12, 87]:

$$B = \frac{8\pi^2}{\lambda c}\int_0^L \frac{n_2}{n_0} I \,\mathrm{d}z\,,$$

where L is the length of the medium. The value of B is the most important characteristic of a specific facility: in the normal operation mode, it should not exceed several units.

The hot debate of the early years as to which of the self-focusing pictures describes the processes in amplifiers — the waveguide picture or that of moving foci — was completely forgotten for about twenty years. Both scenarios lead to the wide-angle scattering of the laser beam upon passing through a nonlinear focus, give rise to a strong spectral broadening due to nonlinear effects in the focal region, and exert a profound effect on the amplification of high-power pulses. Therefore, self-focusing in amplifying media proved to exert a strongly adverse effect with regard to the issue of maximizing laser pulse power, and all investigations in the 1970s–1980s were performed under the slogan of suppressing it.

Different approaches were suggested to reduce the adverse effect of SSSF [12, 84, 86]: the use of apodizing apertures to decrease diffraction-induced perturbations, diverging beams to suppress self-focusing as a whole, circular polarization to decrease the nonlinearity coefficient in the medium, division of the amplifying medium into short segments with air gaps between them for filtering the beam, spatial filters for suppressing small-scale intensity fluctuations in the beam section, and, lastly, the use of active media with a high gain coefficient. The use of wide-aperture disk amplifiers turned out to be the most efficient: the beam intensity was decreased by increasing the beam diameter to several dozen centimeters with a telescope placed in front of the amplifier, which permitted suppressing SSSF in the active medium [88]. In this case, small-scale perturbations of the light field in the beam section were filtered between the stages of a disk amplifier.[5]

The suppression of self-focusing in femtosecond systems, which have a fair chance of achieving a record high power without damaging the active medium, turned out to be the most serious problem. It was clear that the most radical method of SSSF suppression involved a substantial decrease in the amplified pulse power by increasing the pulse duration. This approach had been formulated by Treacy in 1968 [68], who proposed the idea to use phase modulation for lengthening the pulse prior to its entry into the amplifiers and to shorten its duration by compensating the introduced modulation upon amplification. This amplification technique was practically demonstrated by Strickland and Mourou in 1985 [90]; since then, this technique has become classical. The amplification technique itself, which involves a stretcher to effect phase modulation of the pulse before the amplifier and a compressor to shorten the pulse after the amplifier, has come to be known as amplification of pulses with linear frequency modulation, or chirped pulse amplification (CPA).

We note that the stretcher–compressor technique in femtosecond laser systems, in essence, is an extension to the temporal coordinate of the idea to broaden the light field localization domain, which is employed in disk amplifiers to lower the intensity in nano- and picosecond laser systems.

3. Filamentation of femtosecond laser pulses

3.1. Earliest papers and modern reviews

The revival of interest in the effect of laser radiation self-focusing, which is now referred to as filamentation,[6] is directly related to progress in the development of high-power femtosecond laser facilities. This has allowed performing experiments with a pulse whose power is much higher than the critical power for self-focusing in air at atmospheric pressure.

In 1995, in the propagation of a collimated titanium–sapphire laser beam with a power of several dozen gigawatts and a duration of 100–250 fs in air, energy localization in thin (80 μm thick) filaments tens of meters long and broadband conical emission were observed in laboratory conditions [91]. This effect, which was recorded in Mourou's laboratory in the USA, came as a surprise, although the self-focusing of a high-power picosecond laser beam in air had been first noted in an experiment with a converging beam in the late 1960s and in the propagation of collimated 1.06 μm radiation over a distance of 25 m [74].

After Mourou, laboratory experiments on the filamentation of collimated femtosecond pulses in air were performed by the French group of Mysyrowicz [93] and the Canadian group of Chin [94, 95]. A filament with a length of over 200 m was recorded for the first time in the propagation of a pulse with a power of 300 GW along an open atmospheric path [96].

Several hundred original papers, reviews [13, 14, 97–101], and a collection of reprinted and modern papers [15] concerned with the effects of self-focusing and the filamentation of femtosecond laser radiation and with analyses of its possible application have been published to date.

3.2 Filamentation and the moving foci model

The authors of the first filamentation experiments noted the significant role of the induced laser plasma in the formation of many-meter-long filaments with a high energy density, but provided different interpretations for the observed effects. In Ref. [91], the formation of an extended filament was ascribed to radiation self-channeling due to the dynamic balance between the Kerr self-focusing in the gas components of the air, on the one hand, and the defocusing in the laser plasma and diffractive divergence, on the other. The first estimates for the peak intensity in a filament and the electron density in the laser plasma were obtained based on the analysis by Javan and Kelley [102], modified for such a balance. The authors of Ref. [93] used the concept of an anti-waveguide structure with a negative on-axis increment of the refractive index produced by the laser plasma and a shell with a positive increment caused by the Kerr nonlinearity of the air. In this case, the filament is a weak leaky mode of the anti-waveguide, which can persist for a length of tens of meters under certain conditions.

The formation of an extended filament with a high energy density is most amply reproduced by the model proposed in Refs [94, 104]. This model generalizes the moving foci model, which was previously developed [39, 40] for pico- and nanosecond pulses, to the case of transient self-focusing of a femtosecond pulse in conditions of nonlinear refraction in the laser-induced plasma. According to the generalized moving foci model, the filament is a continuous set of nonlinear foci in temporal pulse slices, beginning with the highest-power one. In this case, the temporal pulse slices, unlike those in the classic model [39], are not independent in the filamentation: the intensity redistribution in them is determined by laser plasma production in the previous slices, in which the intensity reached the photoionization threshold due to self-focusing. In the filamentation, the Kerr nonlinearity prevails at the leading edge of the pulse, while the pulse trailing edge is

[5] At present, wide-aperture amplifiers are used in laser fusion facilities in which megawatt nanosecond pulses trigger fusion reactions in a deuterium–tritium plasma [89].

[6] The term 'filamentation' was already used in the first papers on self-focusing, for instance, in Ref. [26].

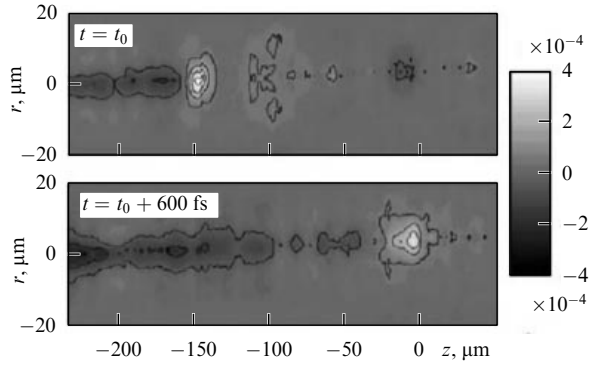

Figure 8. Gray-scale side images of the refractive index increments of water caused by the Kerr (light tone) and plasma (dark tone) nonlinearities in the filamentation of a 120 fs long pulse. The two images, shifted by 600 fs in time, were obtained by the shadow technique with a spatial resolution of 1.5 μm and a temporal resolution of 23 fs [103].

dominated by the plasma nonlinearity, which gives rise to defocusing in the temporal slices that follow the focused ones.

The onset of filamentation is determined by the self-focusing of the temporal slice with a peak pulse power P_{peak}, and the distance to the start of the filament can be calculated by formula (2) or the Marburger formula.[7]

In the filamentation, the increase in the light field intensity in the nonlinear focus is limited not by two-photon absorption in the medium, as implied by the classical moving foci model [39], but by defocusing in the laser plasma [104].[8] The clamping of intensity in a filament results from the dynamic balance between the optical powers of the focusing Kerr lens and defocusing plasma lens [106].

The first estimates of the peak intensity in the filamentation in air, which were made in Ref. [107] assuming that the increments of the refractive index due to the Kerr and plasma nonlinearities were equal, were subsequently confirmed by experiments and theoretical calculations. For a pulse at a wavelength of 800 nm, the peak intensity in the filament is equal to about $10^{13}-10^{14}$ W cm^{-2}, the energy density ~ 0.6 J cm^{-2}, the filament diameter ~ 100 μm, the peak free-electron density of the laser-induced plasma $\sim 10^{14}-10^{16}$ cm^{-3}, and the plasma channel diameter ~ 50 μm. In this case, the intensity is almost independent of the wavelength λ, while the transverse size of the filament and plasma channel vary proportionally to λ and the electron density $\propto \lambda^{-2}$ [108]. In condensed media, for a wavelength of 800 nm, the filament and plasma channel diameters lie in the respective ranges 10–20 μm and 2–5 μm (Fig. 8).

The light field that diverges from the filament axis due to defocusing in the plasma interferes with the light field in the background of the filament to form annular intensity distribution structures around it (Fig. 9), like those observed in the stationary self-focusing in carbon disulphide [33]. The formation of rings in the energy density distribution around a femtosecond filament in air was first recorded in Ref. [109] and interpreted in Ref. [110].

The loss of laser energy in the filamentation is small; it is determined only by the photoionization of the air. That is why the light field defocused in the plasma again contracts to the axis due to Kerr self-focusing to increase the energy density on the filament axis. The effect of refocusing in the filament, which was discovered in Ref. [94] as a nonmonotonic energy density variation along the filament, significantly affects the spatio-temporal evolution of the light field in its propagation. As shown in Ref. [111], for a peak pulse power only slightly higher than the critical self-focusing power, the beam propagation is similar to the self-channeling regime, which was discussed by Askar'yan [112] at the dawn of research on beam self-focusing. In this regime, an extended continuous domain with high energy and electron densities forms, while for a pulse with a high peak power, the filament decays as a result of multiple events of plasma-induced defocusing and subsequent refocusing, into a sequence of isolated pockets of plasma and domains with a high density of the light field.

Initially, the generalized moving foci model did not gain support, and Mysyrowicz's group set up a dedicated experiment on the filamentation of a focused femtosecond pulse for

[7] These formulas are applicable when the effect of group velocity dispersion on the radiation filamentation is negligible.

[8] In the self-focusing in condensed media, the limitation of intensity growth caused by avalanche ionization was reported earlier, for instance, in Ref. [105].

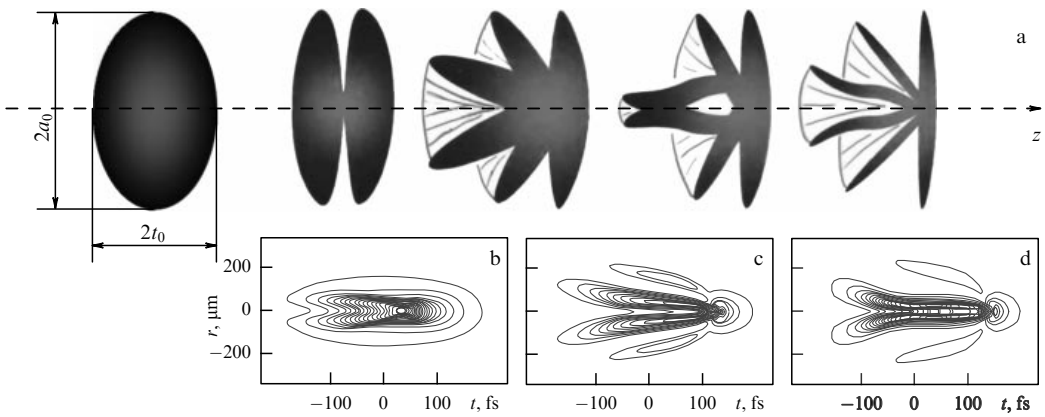

Figure 9. (a) Qualitative picture of variation of the intensity distribution in the plane parallel to the direction of pulse propagation. Computer-calculated lines of equal intensity at distances (b) $z = 27$ m, (c) 33 m, (d) 40 m in the (r, t) plane parallel to the direction of pulse propagation, which illustrate the formation of rings around the filament and the refocusing effect. The peak power is $P_{\text{peak}} = 5P_{\text{cr}}$, where $P_{\text{cr}} = 6$ GW is the critical power for self-focusing in air, the beam radius is 3.5 mm. The interval between the lines of equal intensity in the (r, t) plane is 0.25×10^{13} W cm^{-2} [104].

the purpose of refuting the model [113]. In this experiment, a filament was recorded behind a focused beam waist, which corresponds to the infinite distance for a collimated beam, and behind the beam waist, according to the classic moving foci model, no self-focusing can occur. But the existence of the filament behind the beam waist does not disprove the generalized moving foci model and is a consequence of the effect of refocusing of the light beam that diverges after the beam waist. To date, the filamentation of focused femtosecond pulses has been comprehensively studied, both experimentally and theoretically [114–116].

The moving foci model is intimately related to the notion of an energy reservoir at the beam periphery, which permits explaining the formation of an extended filament as the continuous set of nonlinear foci produced in the contraction of the light field of the whole transverse beam section in temporal slices at the pulse leading edge. In the experiments in Refs [117, 118] with an aperture that transmitted a thin filament and intercepted the beam periphery, no filamentation was recorded after the aperture, which confirms the decisive role of the energy reservoir in the formation of a long-distance filament. The mechanism of dynamic spatial replenishment in the filamentation, which was proposed in Ref. [119], is close to the moving foci model.

3.3 Multiple filamentation and SSSF

Pulses whose power is tens of times the critical self-focusing power produce a multitude of filaments, which owe their origin to SSSF of the high-intensity light field (Fig. 10). In this case, lengthy narrow domains with a high energy density are not continuous along the entire filamentation length. Around the filaments originating from perturbations of the output beam of the laser system, diverging annular structures form, which interfere to produce perturbations for the formation of daughter filaments (Fig. 11). Owing to the energy competition between the filaments, a part of them vanishes, while the remaining ones give rise to the next generation of filaments [120, 121]. As a result, multiple filamentation generates a dynamic set of extended domains with a high energy density and plasma channels. As a rule, their positions in the beam cross section vary randomly in laser beam propagation. According to a recent research into the filamentation of laser pulses with a power of 100 TW in air [122], the filament number density in the beam section saturates with increasing power due to a strong interaction between the filaments.

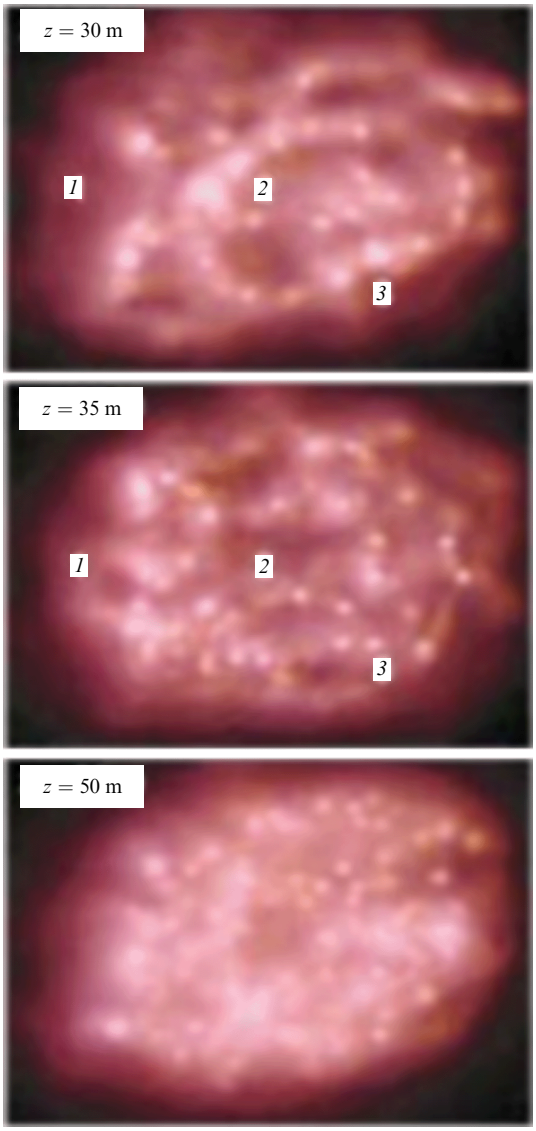

Figure 10. Energy density distribution in the cross section of a 800 nm pulse with the duration 85 fs, the energy 230 mJ, and the peak power 2.3 TW ($\approx 700P_{cr}$) in filamentation in air. Hot spots 1–3, which define the filaments at the distance $z = 30$ m, are caused by initial perturbations, and at a distance of 35 m are caused by secondary filaments, which increase sharply in number at the distance $z = 50$ m [120].

3.4 Nonlinear optics of filaments

The filament of a femtosecond pulse produces a dynamic guiding structure in the bulk of a transparent dielectric, which effects spatial filtering and extracts the fundamental self-focusing mode — the Townes mode [18]. The large filament length, the high energy density, and the femtosecond period of light–medium interaction provide conditions for an efficient nonlinear-optical conversion without recourse to special optical systems. "Nonlinear filamentation optics" [123] involves the superbroadening of the frequency–angle pulse spectrum, the generation of higher-order harmonics and terahertz emission, pulse compression, filament-induced optical anisotropy, and other nonlinear optical effects that accompany the phenomenon of femtosecond filamentation.

In air, the frequency spectrum of the supercontinuum, generated in the femtosecond filamentation, extends from the ultraviolet to near-infrared ranges. The supercontinuum emission band of a 35 fs long terawatt pulse extends from 0.5 μm to 4.5 μm [124]. Conical emission in the anti-Stokes domain of the supercontinuum was recorded in the first experiments on the filamentation of femtosecond pulses in air [90, 92, 94], just as had been observed earlier in the self-focusing in condensed media, for instance, in Ref. [60].

Generalizing the experimental data suggests that in condensed media, spectrum broadening to the anti-Stokes domain depends only on the ratio between the material band gap E_g and the photon energy $h\nu$ of the radiation, and the broadening increases as this ratio increases [125]. The generation threshold for anti-Stokes supercontinuum components is defined by the condition $E_g/(h\nu) \geqslant 2$ [126]. Spectrum superbroadening in the filamentation results from the phase self-modulation of the light field and is determined by both Kerr and plasma nonlinearities, whose responses are

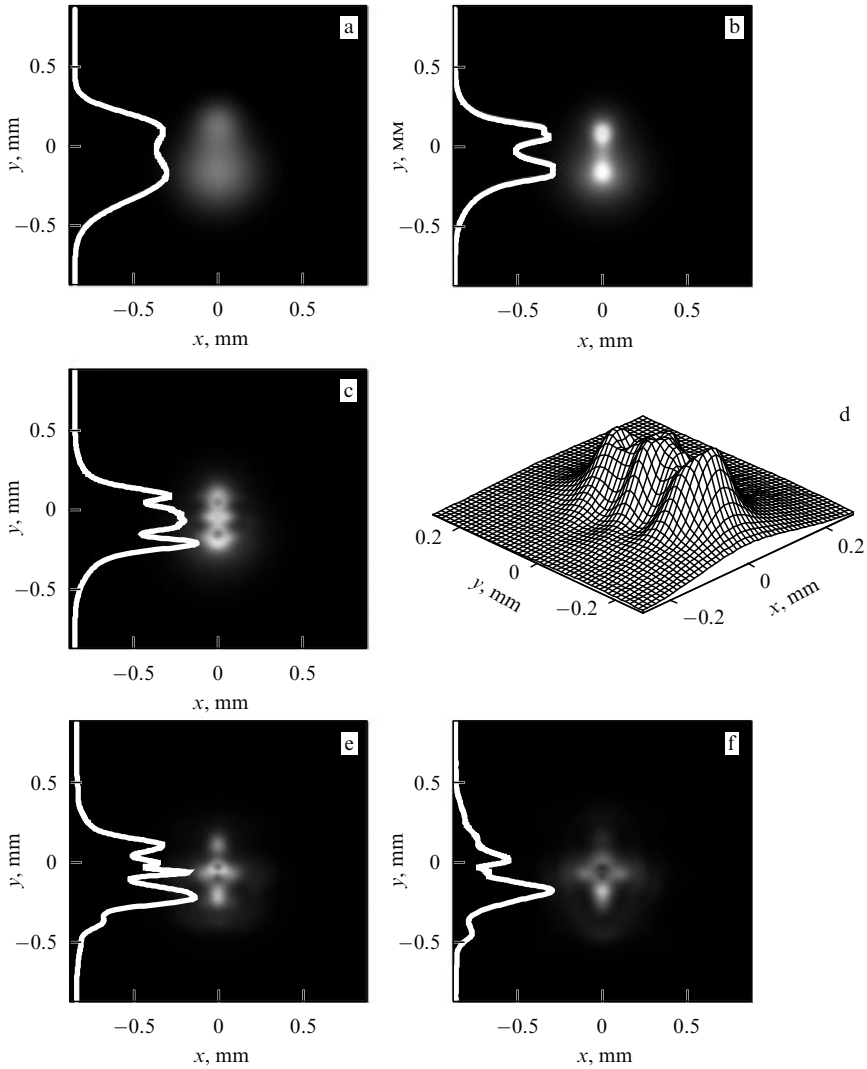

Figure 11. Picture of multiple filamentation formation in the propagation through water for a pulse with the duration 42 fs and the peak power $P_{\text{peak}}/P_{\text{cr}} = 4$: (a) initiation and (b) formation of primary filaments, (c, d) appearance of daughter filaments, and (e, f) onset of competition between the filaments [121].

inherently transient in the femtosecond duration range. The broadening of the frequency spectrum is determined by the time gradient of the nonlinear phase of the light field and the broadening of the angular spectrum by its spatial gradient [127]. [9] The generation of high-intensity anti-Stokes components in a broad spectral band is caused by the 'optical shock wave' formed in the medium with an increase in steepness of the pulse trailing edge due to wave nonstationarity [16, 54] in conditions of pulse compression in space and time. The generation of low-frequency spectrum components occurs primarily in the pulse leading edge. That is why the long-wavelength wing of the supercontinuum is recorded in the form of an axially symmetric peak on the axis and a short-wavelength one in the form of concentric rings of conical emission.

The supercontinuum emission is coherent [128], and its interference is the cause of the emergence of a fine structure of the spectrum in the pulse decay to subpulses and distributed supercontinuum source formation in a lengthy filament [129]. In the pulse refocusing, a sequence of supercontinuum sources forms in the filament, and their radiation interference has the effect that the continuum spectrum of conical emission splits into a multitude of discrete rings [130] (Fig. 12).

The superbroadening of the frequency spectrum of a femtosecond pulse in the filamentation opens possibilities for obtaining ultrashort pulses directly in the bulk of the medium. The use of argon cells for broadening the pulse spectrum in filamentation conditions and of mirrors for the subsequent pulse compression allowed squeezing the pulses and shortening their duration from 42 fs at a wavelength of 800 nm to 5.7 fs with an energy conversion efficiency of 45% [131]. There is a domain in a filament in which the pulse experiences the greatest compression in conditions of normal dispersion. Using this property, for the optimally selected filament length in air, it is possible to shorten the duration of an 800 nm pulse from 55 fs to 9 fs [132].

To interpret the filamentation effect, the concept of X waves (see, e.g., Ref. [133]) was developed, which represents femtosecond laser radiation in the form of a packet of conical waves. The near-field intensity in the radial-coordinate and time variables and the far-field intensity in the divergence

[9] In Ref. [93], the conical emission is interpreted as Cherenkov radiation arising in the dynamic waveguide structure of a lengthy filament.

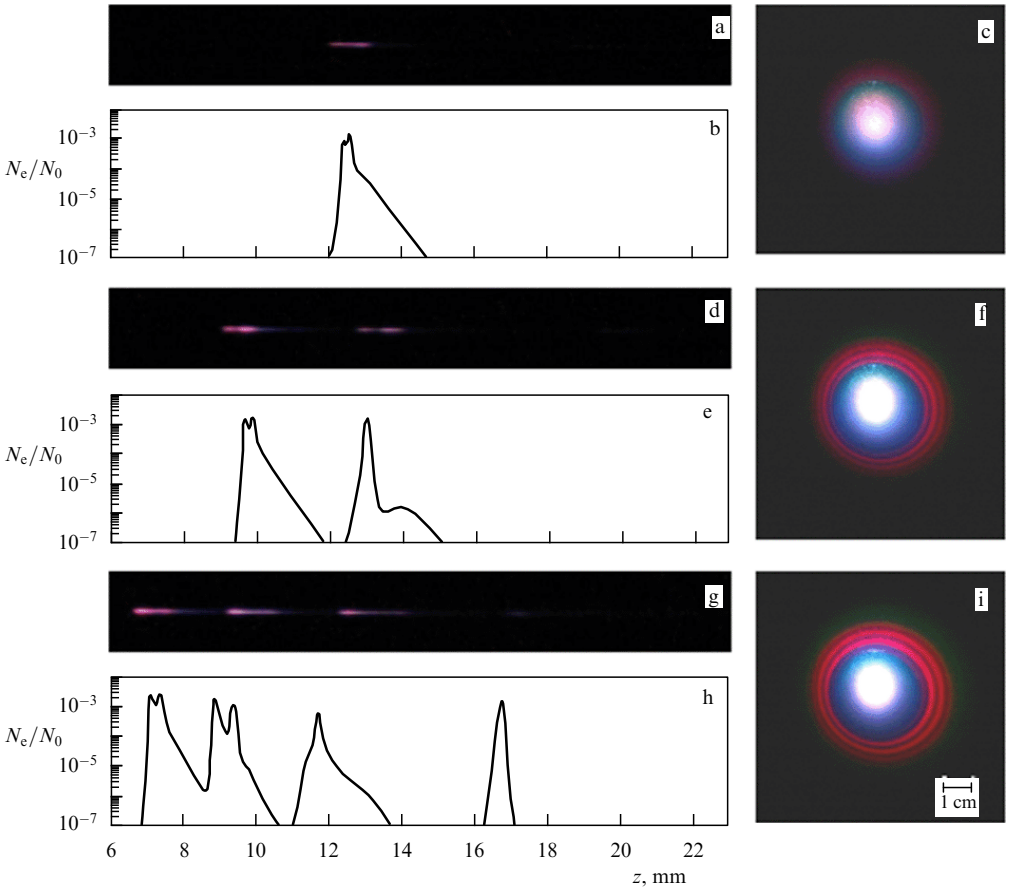

Figure 12. Splitting of conical emission rings in the filamentation of a 35 fs long (FWHM) pulse with a wavelength of 800 nm in a fused quartz sample. (a, d, g) Plasma channels recorded with a camera through a side face of the sample. (b, e, h) Numerically obtained electron density N_e/N_0 (where $N_0 = 2.2 \times 10^{22}$ cm^{-3}) on the axis of the plasma channels. (c, f, i) Conical emission images recorded with a camera. Pulse energies: (a–c) 1.5 μJ, (d–f) 1.9 μJ, (g–i) 2.4 μJ [130].

angle and wavelength variables have a characteristic X-like shape in the filamentation in a medium with a normal dispersion.

In the filamentation, a nonlinear phase matching occurs between the fundamental and third harmonic radiation, with the consequence that the coherent conversion length is much longer than in air [134]. However, the conversion efficiency is not high (0.1–0.2 %) because of the pulse intensity limitation in a filament. Several experiments have demonstrated the feasibility of generating higher-order harmonics in the laser plasma of a femtosecond filament. In xenon at a pressure of 50 mbar, it was possible to record the generation of harmonics of 800 nm radiation up to the 15th order [135], and in helium at a pressure of 100 mbar, the generation of 45th to 91st-order harmonics was recorded [136].

Emission of the terahertz frequency range in a filament plasma channel was first recorded in air in [137]. More recently, it was discovered that the higher-intensity terahertz emission propagated forward at a small angle of deviation from the filament axis and was radially polarized irrespective of the laser pulse polarization [138]. According to the most widely accepted model, the sources of terahertz emission are the currents in the laser-induced plasma, which arise under the action of ponderomotive forces and propagate together with the pulse [139]. Under a 'two-color' action on the plasma by laser pulses, at the fundamental frequency and its second harmonic, the efficiency of terahertz emission generation increases significantly for a certain phase relation between the acting harmonics [140, 141].

3.5 Applications of femtosecond filamentation

The concentration of laser radiation energy in a long-distance filament, the generation of a supercontinuum, terahertz emission and plasma channels, and other effects accompanying femtosecond filamentation immediately attracted the attention of researchers by their possible practical applications. For example, we note energy delivery over kilometer-long distances to obtain optical breakdown plasmas and a fluorescence signal, the remote monitoring of pollutants, laser-assisted broadband probing of the environment, the use of femtosecond plasma filament channels for directional microwave radiation transfer, and the fabrication of micro-optical elements.

The greatest success in investigations of the practical application of femtosecond filamentation in atmospheric optics was achieved in the French–German Teramobile project (www.teramobile.org), the first reports about it dating back to 2000 [142].

The mobile Teramobile system accommodated in a conventional cargo container contains a terawatt laser with the following output parameters: 793 nm wavelength, 16 nm spectral bandwidth, 70 fs pulse duration, the energy 350 mJ, the peak power 5 TW, the repetition rate 10 Hz, and the output beam diameter 50 mm. The system comprises

telescopes for directing the laser beam along horizontal and vertical paths, a receiving telescope with an aperture of 40 cm, and a recording system with spectrometers with the total bandwidth ranging from 190 nm to 2.5 μm.

The mobility of the high-power femtosecond system allowed realizing several unique field and large-scale laboratory experiments to comprehensively investigate both the effect of high-power laser pulse filamentation in the real conditions of extended atmospheric paths and the applied aspects of this effect. Recorded in these experiments were 'hot spots' with a high energy density at a distance of more than 2 km and plasma channels up to 400 m in length; the feasibility of using the supercontinuum emission of a femtosecond filament for broadband laser probing was demonstrated by the example of water absorption spectra obtained from an altitude of 4.5 km. Furthermore, remote diagnostics of a bioaerosol were implemented, fluorescence spectra were recorded in the breakdown initiated by the filament on the surface of a 180 m distant target, and the filament plasma was found to lower the threshold of a high-voltage electric discharge and to exert a guiding action on it.

In an experiment carried out under the auspices of the Langmuir Laboratory for Atmospheric Research (USA), a correlation was recorded between the radio-frequency pulses arising from lightning discharges and the formation of femtosecond filaments in the atmosphere [13, 14, 98–101, 124].

By analyzing experimental data, the authors of [143, 144] reached the conclusion that fluorescence initiated by a femtosecond filament can be used for the remote detection and identification of chemical and biological pollutants in the atmosphere, as well as for the spectral analysis of remote targets.

The idea of using laser plasmas for the transmission of microwave radiation, which was expressed in Ref. [145], was elaborated by the authors of Ref. [146], who proposed forming a virtual microwave waveguide from a bunch of plasma channels produced in the filamentation of femtosecond laser pulses in air. The optimal configurations of the bunch of plasma channels, which form a cylindrical waveguide for a microwave pulse in multiple femtosecond filamentation, were theoretically investigated in Ref. [147]. Directional microwave energy transfer along a cylindrical plasma waveguide was experimentally realized in Ref. [148] with a laser array equipped with an adaptive mirror for the formation of an annular bunch of plasma channels, which were produced by more than 1000 filaments in the propagation of pulsed 27 fs long, 800 nm radiation with an energy of 1.5 J through the air.

The use of pulsed near-infrared laser radiation for the micromodification of optical materials was first demonstrated in Ref. [149]. Waveguides, optical couplers, bulk diffraction gratings, phase transparencies, and other elements of microoptics were fabricated in the bulk of optical glasses with the help of femtosecond filaments.

With the development of laser technologies involving filamentation, the problem of controlling filamentation in order to optimize the parameters of laser radiation and laser-induced plasma in specific conditions has increased in importance. This control can be exerted only by varying the initial laser pulse parameters to affect the initial filamentation stage, which is determined by nonstationary self-focusing of the pulse. Therefore, controlling filamentation and nonstationary self-focusing of pulsed laser beams constitutes a unitary task for nonlinear optics.

4. Conclusions

The common laws of the effects of the self-focusing of light beams and filamentation of laser pulses reflect the common physical nature of these effects. Progress in the studies of beam self-focusing in the 1960s–1970s (see reviews [3, 112, 150–152] as well as Refs [2, 15, 85, 153–163]) laid the foundation for the rapid progress in investigating the filamentation of laser pulses, beginning from the 1990s. After the discovery of self-focusing, the hopes of the early years for an effective solution to the problem of long-distance transfer of laser energy yielded to disappointment. It is likely that only the USP formation in the course of light field scattering with self-focusing in the active medium has found practical application in femtosecond pulse oscillators. At present, the development of femtosecond laser technologies involving laser pulse filamentation is becoming a reality.

Acknowledgements
This work was supported by the Russian Foundation for Basic Research, Grant No. 11-02-00556a. S V Ch expresses his appreciation to E A Vinogradov's scientific school, NSh-1049.2012.2, and V P K acknowledges support from Grant No. NSh-6897.2012.2 from the President of Russian Federation.

References

1. Askar'yan G A *Sov. Phys. JETP* **15** 1088 (1962) [*Zh. Eksp. Teor. Fiz.* **42** 1567 (1962)]
2. Shen Y R *The Principles of Nonlinear Optics* (New York: J. Wiley, 1984) [Translated into Russian (Moscow: Nauka, 1989)]
3. Akhmanov S A, Sukhorukov A P, Khokhlov R V *Sov. Phys. Usp.* **10** 609 (1968) [*Usp. Fiz. Nauk* **93** 19 (1967)]
4. Kasparian J, Béjot P, Wolf J-P *Opt. Lett.* **35** 2795 (2010)
5. Wahlstrand J K et al. *Phys. Rev. Lett.* **107** 103901 (2011)
6. Kosareva O et al. *Opt. Lett.* **36** 1035 (2011)
7. Vlasov S N, Koposova E V *Radiophys. Quantum Electron.* **54** 185 (2011) [*Izv. Vyssh. Uchebn. Zaved., Radiofiz.* **54** 207 (2011)]
8. Bolotovskii B M, in *Pamyati G A Askar'yana* (Commemorating G A Askar'yan) (Comp. G M Batanov et al.) (Moscow: Fizmatlit, 2000)
9. Landau L D, Lifshitz E M *Electrodynamics of Continuous Media* (Oxford: Pergamon Press, 1984) [Translated from Russian: *Elektrodinamika Sploshnykh Sred* (Moscow: Nauka, 1982)]
10. Vinogradova M B, Rudenko O V, Sukhorukov A P *Teoriya Voln* (The Theory of Waves) (Moscow: Nauka, 1979)
11. Vlasov S N, Talanov V I *Samofokusirovka Voln* (Wave Self-Focusing) (Nizhny Novgorod: Institut Prikladnoi Fiziki RAN, 1997)
12. Mak A A et al. *Lazery na Neodimovom Stekle* (Neodymium Glass Lasers) (Moscow: Nauka, 1990)
13. Chin S L *Femtosecond Laser Filamentation* (New York: Springer, 2010)
14. Kandidov V P, Shlenov S A, in *Glubokoe Kanalirovanie i Filamentatsiya Moshchnogo Lazernogo Izlucheniya v Veshchestve* (Deep Channeling and Filamentation of Laser Radiation in Substance) (Ed. V Ya Panchenko) (Moscow: Interkontakt Nauka, 2009) p. 185
15. Boyd R W, Lukishova S G, Shen Y R (Eds) *Self-focusing. Past and Present. Fundamentals and Prospects* (Topics in Applied Physics, Vol. 114) (New York: Springer, 2009)
16. Akhmanov S A, Vysloukh V A, Chirkin A S *Optics of Femtosecond Laser Pulses* (New York: American Institute of Physics, 1992) [Translated from Russian: *Optika Femtosekundnykh Lazernykh Impul'sov* (Moscow: Nauka, 1988)]
17. Talanov V I *Sov. Radiophys.* **7** 254 (1964) [*Izv. Vyssh. Uchebn. Zaved. Radiofiz.* **7** 564 (1964)]
18. Chiao R Y, Garmire E, Townes C H *Phys. Rev. Lett.* **13** 479 (1964)

19. Sukhorukov A P, in *Fizicheskaya Entsiklopediya* (Encyclopedia of Physics) (Ed. A M Prokhorov) (Moscow: Bol'shaya Rossiiskaya Entsiklopediya, 1994) p. 415
20. Vlasov S N, Petrishchev V A, Talanov V I *Radiophys. Quantum Electron.* **14** 1062 (1974) [*Izv. Vyssh. Uchebn. Zaved. Radiofiz.* **14** 1353 (1971)]
21. Fibich G, Gaeta A L *Opt. Lett.* **25** 335 (2000)
22. Kandidov V P, Fedorov V Yu *Quantum Electron.* **34** 1163 (2004) [*Kvantovaya Elektron.* **34** 1163 (2004)]
23. Talanov V I *Sov. Radiophys.* **9** 260 (1966) [*Izv. Vyssh. Uchebn. Zaved. Radiofiz.* **9** 410 (1966)]
24. Hercher M *J. Opt. Soc. Am.* **54** 563 (1964)
25. Chiao R Y, Gustafson T K, Kelley P L, in *Self-focusing. Past and Present. Fundamentals and Prospects* (Topics in Applied Physics, Vol. 114, Eds R W Boyd, S G Lukishova, Y R Shen) (New York: Springer, 2009) p. 129
26. Pilipetskii N F, Rustamov A R *JETP Lett.* **2** 55 (1965) [*Pis'ma Zh. Eksp. Teor. Fiz.* **2** 88 (1965)]
27. Lallemand P, Bloembergen N *Phys. Rev. Lett.* **15** 1010 (1965)
28. Kelley P L *Phys. Rev. Lett.* **15** 1005 (1965)
29. Gol'dberg V N, Talanov V I, Erm R E *Radiophys. Quantum Electron.* **10** 368 (1967) [*Izv. Vyssh. Uchebn. Zaved. Radiofiz.* **10** 674 (1967)]
30. Marburger J H *Prog. Quantum Electron.* **4** 35 (1975)
31. Vlasov S N *Sov. J. Quantum Electron.* **17** 1191 (1987) [*Kvantovaya Elektron.* **14** 1868 (1987)]
32. Vysotina N V et al. *Opt. Spectrosc.* **98** 895 (2005) [*Opt. Spektrosk.* **98** 976 (2005)]
33. Garmire E, Chiao R Y, Townes C H *Phys. Rev. Lett.* **16** 347 (1966)
34. Akhmanov S A, Sukhorukov A P, Khokhlov R V *Sov. Phys. JETP* **23** 1025 (1966) [*Zh. Eksp. Teor. Fiz.* **50** 1537 (1966)]
35. Khokhlov R V, in *Tezisy Dokladov I Vsesoyuz. Simpoziuma po Nelineinoi Optike* (Abstracts of Reports to the Ist All-Union Symp. on Nonlinear Optics) (Minsk, 1966)
36. Bespalov V I, Talanov V I *JETP Lett.* **3** 307 (1966) [*Pis'ma Zh. Eksp. Teor. Fiz.* **3** 471 (1966)]
37. McWane P D *Nature* **211** 1081 (1966)
38. Marburrger J H, Wagner W G *IEEE J. Quantum Electron.* **3** 415 (1967)
39. Dyshko A L, Lugovoi V N, Prokhorov A M *JETP Lett.* **6** 146 (1967) [*Pis'ma Zh. Eksp. Teor. Fiz.* **6** 655 (1967)]
40. Lugovoi V N, Prokhorov A M *JETP Lett.* **7** 117 (1968) [*Pis'ma Zh. Eksp. Teor. Fiz.* **7** 153 (1968)]
41. Giuliano C R, Marburger J H *Phys. Rev. Lett.* **27** 905 (1971)
42. Korobkin V V et al. *JETP Lett.* **11** 94 (1970) [*Pis'ma Zh. Eksp. Teor. Fiz.* **11** 153 (1970)]
43. Loy M M T, Shen Y R *Phys. Rev. Lett.* **22** 994 (1969)
44. Chaban A A *JETP Lett.* **5** 48 (1967) [*Pis'ma Zh. Eksp. Teor. Fiz.* **5** 61 (1967)]
45. Nayyar V P, Kumar A *Opt. Commun.* **73** 501 (1989)
46. Vlasov S N et al. *Radiophys. Quantum Electron.* **21** 358 (1978) [*Izv. Vyssh. Uchebn. Zaved. Radiofiz.* **21** 521 (1978)]
47. Golubkov A A, Makarov V A *Radiophys. Quantum Electron.* **31** 737 (1988) [*Izv. Vyssh. Uchebn. Zaved. Radiofiz.* **31** 1042 (1988)]
48. Golubkov A A, Makarov V A, Perezhogin I A *Moscow Univ. Phys. Bull.* **64** (1) 54 (2009) [*Vestn. Mosk. Gos. Univ. Ser. 3 Fiz. Astron.* (1) 49 (2009)]
49. Makarov V A, Perezhogin I A, Potravkin N N *Laser Phys.* **19** 322 (2009)
50. Golubkov A A, Makarov V A, Rakhmatullina I G *Sov. J. Quantum Electron.* **22** 1117 (1992) [*Kvantovaya Elektron.* **19** 1195 (1992)]
51. Makarov V A, Perezhogin I A, Potravkin N N *Opt. Spectrosc.* **109** 778 (2010) [*Opt. Spektrosk.* **109** 839 (2010)]
52. Bloembergen N, Lallemand P *Phys. Rev. Lett.* **16** 81 (1966)
53. Shimizu F *Phys. Rev. Lett.* **19** 1097 (1967)
54. Joenk R J, Landauer R *Phys. Lett. A* **24** 228 (1967)
55. Ostrovskii L A *Sov. Phys. Tech. Phys.* **8** 679 (1964) [*Zh. Tekh. Fiz.* **33** 905 (1963)]
56. Ostrovskii L A *Sov. Phys. JETP* **24** 797 (1967) [*Zh. Eksp. Teor. Fiz.* **51** 1189 (1966)]
57. Bondarenko N G, Eremina I V, Talanov V I *JETP Lett.* **12** 85 (1970) [*Pis'ma Zh. Eksp. Teor. Fiz.* **12** 125 (1970)]
58. Alfano R R, Shapiro S L *Phys. Rev. Lett.* **24** 592 (1970)
59. Alfano R R, Shapiro S L *Phys. Rev. Lett.* **24** 584 (1970)
60. Alfano R R, Hope L L, Shapiro S L *Phys. Rev. A* **6** 433 (1972)
61. Il'ichev N N et al. *JETP Lett.* **15** 133 (1972) [*Pis'ma Zh. Eksp. Teor. Fiz.* **15** 191 (1972)]
62. Smith W L, Liu P, Bloembergen N *Phys. Rev. A* **15** 2396 (1977)
63. Bloembergen N *Opt. Commun.* **8** 285 (1973)
64. Corkum P B, Rolland C, Srinivasan-Rao T *Phys. Rev. Lett.* **57** 2268 (1986)
65. Alfano R R, Shapiro S L *Chem. Phys. Lett.* **8** 631 (1971)
66. Letokhov V S *Sov. Phys. JETP* **28** 1026 (1969) [*Zh. Eksp. Teor. Fiz.* **55** 1943 (1968)]
67. Kuznetsova T I *Sov. Phys. JETP* **30** 904 (1970) [*Zh. Eksp. Teor. Fiz.* **57** 1673 (1969)]
68. Fleck J A *Appl. Phys. Lett.* **12** 178 (1968)
69. Treacy E B *Phys. Lett. A* **28** 34 (1968)
70. Glenn W H, Brienza M J *Appl. Phys. Lett.* **10** 221 (1967)
71. Basov N G et al. *Sov. Phys. JETP* **33** 289 (1971) [*Zh. Eksp. Teor. Fiz.* **60** 533 (1971)]
72. Bykovskii N E et al. *Sov. J. Quantum Electron.* **2** 56 (1972) [*Kvantovaya Elektron.* **7** 68 (1972)]
73. Malyutin A A, Shchelev M Ya *JETP Lett.* **9** 266 (1969) [*Pis'ma Zh. Eksp. Teor. Fiz.* **9** 445 (1969)]
74. Korobkin V V, Malyutin A A, Shchelev M Ya *JETP Lett.* **11** 103 (1970) [*Pis'ma Zh. Eksp. Teor. Fiz.* **11** 168 (1970)]
75. Basov N G et al. *Sov. Phys. JETP* **30** 641 (1970) [*Zh. Eksp. Teor. Fiz.* **57** 1175 (1969)]
76. Basov N G et al. *Sov. Phys. JETP* **38** 449 (1974) [*Zh. Eksp. Teor. Fiz.* **65** 907 (1973)]
77. Korobkin V V, Malyutin A A, Prokhorov A M *JETP Lett.* **12** 150 (1970) [*Pis'ma Zh. Eksp. Teor. Fiz.* **12** 216 (1970)]
78. Zherikhin A N et al. *Sov. Phys. JETP* **39** 52 (1974) [*Zh. Eksp. Teor. Fiz.* **66** 116 (1974)]
79. Zherikhin A N et al. *Sov. J. Quantum Electron.* **4** 525 (1974) [*Kvantovaya Elektron.* **1** 956 (1974)]
80. Spence D E, Kean P N, Sibbett W *Opt. Lett.* **16** 42 (1991)
81. Brabec T et al. *Opt. Lett.* **17** 1292 (1992)
82. Kryukov P G *Quantum Electron.* **31** 95 (2001) [*Kvantovaya Elektron.* **31** 95 (2001)]
83. Lozhkarev V V et al. *Laser Phys. Lett.* **4** 421 (2007)
84. Zherikhin A N, Matveets Yu A, Chekalin S V *Sov. J. Quantum Electron.* **6** 858 (1976) [*Kvantovaya Elektron.* **3** 1585 (1976)]
85. Baranova N B et al. *J. Sov. Laser Res.* **1** 62 (1980) [*Trudy Fiz. Inst. Akad. Nauk* **103** 84 (1978)]
86. Askar'yan G A, Diyanov Kh A, Mukhamadzhanov M *JETP Lett.* **16** 149 (1972) [*Pis'ma Zh. Eksp. Teor. Fiz.* **16** 211 (1972)]
87. Lukishova S G, in *Self-focusing. Past and Present. Fundamentals and Prospects* (Topics in Applied Physics, Vol. 114, Eds R W Boyd, S G Lukishova, Y R Shen) (New York: Springer, 2009) p. 191
88. Baranova N B et al. *Sov. J. Quantum Electron.* **4** 1362 (1975) [*Kvantovaya Elektron.* **1** 2450 (1974)]
89. Moses E I *Nucl. Fusion* **49** 104022 (2009)
90. Strickland D, Mourou G *Opt. Commun.* **56** 219 (1985)
91. Braun A et al. *Opt. Lett.* **20** 73 (1995)
92. Korobkin V V, Alcock A J *Phys. Rev. Lett.* **21** 1433 (1968)
93. Nibbering E T J et al. *Opt. Lett.* **21** 62 (1996)
94. Brodeur A et al. *Opt. Lett.* **22** 304 (1997)
95. Kosareva O G et al. *Opt. Lett.* **22** 1332 (1997)
96. La Fontaine B et al. *Phys. Plasmas* **6** 1615 (1999)
97. Chin S L et al. *Can. J. Phys.* **83** 863 (2005)
98. Couairon A, Mysyrowicz A *Phys. Rep.* **441** 47 (2007)
99. Bergé L et al. *Rep. Prog. Phys.* **70** 1633 (2007)
100. Kasparian J, Wolf J-P *Opt. Express* **16** 466 (2008)
101. Kandidov V P, Shlenov S A, Kosareva O G *Quantum Electron.* **39** 205 (2009) [*Kvantovaya Elektron.* **39** 205 (2009)]
102. Javan A, Kelley P *IEEE J. Quantum Electron.* **2** 470 (1966)
103. Minardi S et al. *Opt. Lett.* **33** 86 (2008)
104. Kosareva O G et al. *J. Nonlin. Opt. Phys. Mater.* **6** 485 (1997)
105. Yablonovitch E, Bloembergen N *Phys. Rev. Lett.* **29** 907 (1972)
106. Kandidov V P et al. *Quantum Electron.* **41** 382 (2011) [*Kvantovaya Elektron.* **41** 382 (2011)]
107. Kasparian J, Sauerbrey R, Chin S L *Appl. Phys. B* **71** 877 (2000)
108. Fedorov V Yu, Kandidov V P *Laser Phys.* **18** 1530 (2008)
109. Chin S L et al. *Opt. Commun.* **188** 181 (2001)

110. Chin S L et al. *Opt. Commun.* **210** 329 (2002)
111. Fedorov V Y, Tverskoy O V, Kandidov V P *Appl. Phys. B* **99** 299 (2010)
112. Askar'yan G A *Sov. Phys. Usp.* **16** 680 (1974) [*Usp. Fiz. Nauk* **111** 249 (1973)]
113. Lange H R et al. *Opt. Lett.* **23** 120 (1998)
114. Théberge F et al. *Phys. Rev. E* **74** 036406 (2006)
115. Ionin A A et al. *JETP Lett.* **90** 423 (2009) [*Pis'ma Zh. Eksp. Teor. Fiz.* **90** 467 (2009)]
116. Geints Yu E, Zemlyanov A A *Atmos. Ocean. Opt.* **23** 270 (2010) [*Opt. Atmos. Okeana* **23** 274 (2010)]
117. Dubietis A et al. *Phys. Rev. Lett.* **92** 253903 (2004)
118. Liu W et al. *Appl. Phys. B* **80** 857 (2005)
119. Mlejnek M, Wright E M, Moloney J V *Opt. Lett.* **23** 382 (1998)
120. Bergé L et al. *Phys. Rev. Lett.* **92** 225002 (2004)
121. Hosseini S A et al. *Phys. Rev. A* **70** 033802 (2004)
122. Henin S et al. *Appl. Phys. B* **100** 77 (2010)
123. Chin S L, Théberge F, Liu W *Appl. Phys. B* **86** 477 (2007)
124. Kasparian J et al. *Science* **301** 61 (2003)
125. Nagura Ch et al. *Appl. Opt.* **41** 3735 (2002)
126. Brodeur A, Chin S L *Phys. Rev. Lett.* **80** 4406 (1998)
127. Kandidov V P et al. *Appl. Phys. B* **77** 149 (2003)
128. Chin S L et al. *J. Nonlin. Opt. Phys. Mater.* **8** 121 (1999)
129. Dormidonov A E, Kandidov V P *Laser Phys.* **19** 1993 (2009)
130. Dormidonov A E et al. *Quantum Electron.* **39** 653 (2009) [*Kvantovaya Elektron.* **39** 653 (2009)]
131. Hauri C P et al. *Appl. Phys. B* **79** 673 (2004)
132. Kosareva O G et al. *Appl. Phys. B* **91** 35 (2008)
133. Faccio D et al. *Phys. Rev. Lett.* **96** 193901 (2006)
134. Aközbek N et al. *Phys. Rev. Lett.* **89** 143901 (2002)
135. Lange H R et al. *Phys. Rev. Lett.* **81** 1611 (1998)
136. Painter J C et al. *Opt. Lett.* **31** 3471 (2006)
137. Tzortzakis S et al. *Opt. Lett.* **27** 1944 (2002)
138. D'Amico C et al. *Phys. Rev. Lett.* **98** 235002 (2007)
139. Sprangle P et al. *Phys. Rev. E* **69** 066415 (2004)
140. Balakin A V et al. *J. Opt. Soc. Am. B* **27** 16 (2010)
141. Bodrov S B et al. *Opt. Express* **19** 6829 (2011)
142. Wille H et al. *Eur. Phys. J. Appl. Phys.* **20** 183 (2002)
143. Chin S L et al. *Appl. Phys. B* **95** 1 (2009)
144. Xu H L, Chin S L *Sensors* **11** 32 (2011)
145. Askar'yan G A *Sov. Phys. JETP* **28** 732 (1969) [*Zh. Eksp. Teor. Fiz.* **55** 1400 (1968)]
146. Valuev V V, Kandidov V P, Cherepenin V A *Integral* (6) 6 (2006)
147. Dormidonov A E et al. *Proc. SPIE* **6733** 67332S (2007)
148. Châteauneuf M et al. *Appl. Phys. Lett.* **92** 091104 (2008)
149. Davis K M et al. *Opt. Lett.* **21** 1729 (1996)
150. Akhmanov S A, Khokhlov R V, Sukhorukov A P, in *Laser Handbook* Vol. 2 (Eds F T Arecchi, E O Schulz-Dubois) (Amsterdam: North-Holland, 1972) p. 1151
151. Lugovoi V N, Prokhorov A M *Sov. Phys. Usp.* **16** 658 (1974) [*Usp. Fiz. Nauk* **111** 203 (1973)]
152. Bespalov V I, Litvak A G, Talanov V I, in *Nelineinaya Optika. Trudy 2-go Vsesoyuz. Simpoziuma po Nelineinoi Optike* (Nonlinear Optics. Proc. of the 2nd All-Union Symp. on Nonlinear Optics) (Ed.-in-Chief R V Khokhlov) (Novosibirsk: Nauka, 1968) p. 428
153. Sukhorukov A P *Sov. Phys. Usp.* **13** 410 (1970) [*Usp. Fiz. Nauk* **101** 81 (1970)]
154. Askaryan G A *Sov. Phys. Usp.* **15** 517 (1973) [*Usp. Fiz. Nauk* **107** 507 (1972)]
155. Zakharov V E *Sov. Phys. Usp.* **15** 518 (1973) [*Usp. Fiz. Nauk* **107** 509 (1972)]
156. Lugovoi V N *Sov. Phys. Usp.* **15** 519 (1973) [*Usp. Fiz. Nauk* **107** 510 (1972)]
157. Korobkin V V *Sov. Phys. Usp.* **15** 520 (1973) [*Usp. Fiz. Nauk* **107** 512 (1972)]
158. Talanov V I *Sov. Phys. Usp.* **15** 521 (1973) [*Usp. Fiz. Nauk* **107** 514 (1972)]
159. Litvak A G *Sov. Phys. Usp.* **15** 523 (1973) [*Usp. Fiz. Nauk* **107** 515 (1972)]
160. Svelto O *Prog. Opt.* **12** 1 (1974)
161. Shen Y R *Prog. Quantum Electron.* **4** 1 (1975)
162. Fleck J A (Jr.), Morris J R, Feit M D *Appl. Phys.* **10** 129 (1976)
163. Manenkov A A *Phys. Usp.* **54** 100 (2011) [*Usp. Fiz. Nauk* **181** 107 (2011)]